

This work was written as part of one of the author's official duties as an Employee of the United States Government and is therefore a work of the United States Government. In accordance with 17 U.S.C. 105, no copyright protection is available for such works under U.S. Law.

Public Domain Mark 1.0

<https://creativecommons.org/publicdomain/mark/1.0/>

Access to this work was provided by the University of Maryland, Baltimore County (UMBC) ScholarWorks@UMBC digital repository on the Maryland Shared Open Access (MD-SOAR) platform.

Please provide feedback

Please support the ScholarWorks@UMBC repository by emailing scholarworks-group@umbc.edu and telling us what having access to this work means to you and why it's important to you. Thank you.

MAGNETOHYDRODYNAMIC TURBULENCE IN THE SOLAR WIND¹

M. L. Goldstein and D. A. Roberts

Code 692, NASA-Goddard Space Flight Center, Greenbelt, Maryland 20771

W. H. Matthaeus

Bartol Research Institute, University of Delaware, Newark, Delaware 19716

KEY WORDS: interplanetary medium, Alfvénic fluctuations, shear instabilities, nonlinear interactions

ABSTRACT

The fluctuations in magnetic field and plasma velocity in the solar wind possess many features expected of fully developed magnetohydrodynamic turbulence. Understanding this nonlinear system is complicated by the dynamical effects of velocity shear between fast and slow solar wind streams, by the spherical expansion of the solar wind, and by its compressibility. Direct spacecraft observations from 0.3 to over 20 AU, radio scintillation observations of plasmas near the Sun, numerical simulations, and various models provide complementary methods that have shown convincingly that the fluctuations in the wind parameters undergo significant dynamical evolution independent of whatever turbulence might exist in the solar photosphere and corona. This rich area of study allows one to test theories of turbulence against direct observation, and to use observations to guide and motivate development of turbulence theories. The solar wind thus provides an excellent laboratory for studying many fundamental questions about turbulent plasmas.

1. INTRODUCTION

Despite the tenuousness of the solar wind at the orbit of Earth (the average density is 5 particles/cm³), its physical parameters can be measured with great

¹The US Government has the right to retain a nonexclusive, royalty-free license in and to any copyright covering this paper.

precision by in situ spacecraft. For example, plasma experiments are able to determine the full, three-dimensional plasma distribution function of electrons, protons, and some ion species while magnetometers and a variety of plasma wave instruments have provided a detailed characterization of the electromagnetic wave fields. The spatial scales sampled by spacecraft and remote sensing techniques range from tens of AU down to a few kilometers, and the sampled temporal scales range from years to fractions of a second. The completeness with which the in situ properties of the solar wind have been characterized has made the heliosphere an excellent laboratory in which to study turbulence in a magnetofluid. These detailed observations have stimulated the development of new analytical techniques and increasingly sophisticated numerical simulations.

The fundamental issue addressed in studies of solar wind turbulence is to ascertain the origin, nature, and dynamics of the fluctuating magnetic and velocity fields. This involves studying large-scale structures (streams) down to the kinetic scale of the ion (and ultimately, electron) Larmor radius. In general terms, the origin of these fluctuations is clear: The Sun's surface and inner atmosphere are time-variable and inhomogeneous. Structures such as coronal holes, striated arches, plumes, helmets, etc continuously appear and fade within seconds, days, or months. Exactly how this activity gives rise to the fluctuating fields observed by spacecraft has proven to be one of the thorniest questions in heliospheric physics, one that remains open despite years of study.

Although high-speed streams drive much of the evolution of the turbulence, the smaller scale solar variability gives rise to both compressive and shear variations in the flow. While much of the compressive component should be rapidly damped, some of the fast-mode waves and most of the nonpropagating, nearly pressure-balanced compressive structures can pass through the corona and enter the solar wind. Propagating incompressive fluctuations are primarily "Alfvénic" fluctuations, which are difficult to damp; it is thus no surprise that they are the major component of solar wind turbulence. The wind flow becomes faster than the Alfvén wave speed ($B/\sqrt{4\pi\rho}$, where B is the magnetic field strength and ρ is the mass density) at a critical point somewhere between 10 and 20 solar radii from the Sun where only outward-propagating Alfvén waves can be convected into the solar wind. Any inward-propagating fluctuations observed in the wind must be generated in situ.

What is observed at 0.3 AU and beyond is a dynamical mixture of Alfvénic fluctuations, convected structures, microstreams, and propagating compressive structures that have all been influenced by the nearly spherical expansion of the flow. This expansion is the dominant influence on the amplitude of the fluctuations. Apart from the expansion, shears between and within streams and the inhomogeneities associated with convected structures interact nonlinearly with the Alfvénic population and with dynamically active two-dimensional

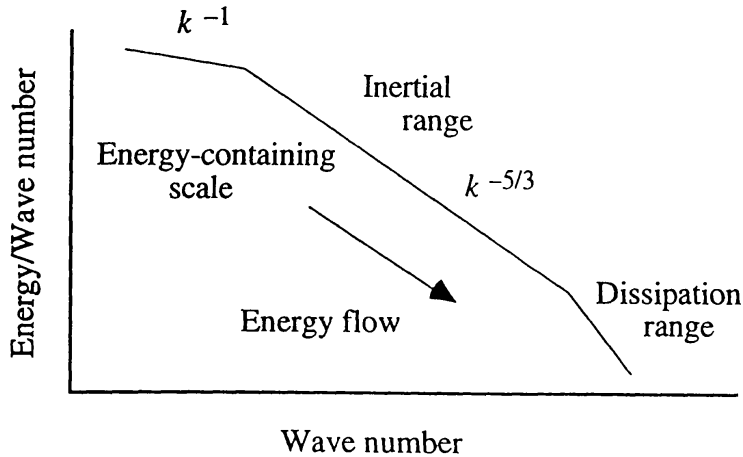


Figure 1 A schematic representation of a power spectrum of either magnetic fluctuations or fluctuations of the total energy of solar wind fields.

fluctuations. The Alfvénic fluctuations, interacting among themselves, can excite compressive fluctuations. They also interact with two-dimensional incompressive fluctuations to produce spectral anisotropies in the incompressible component of the flow—especially a transfer to higher wave numbers perpendicular to the large-scale magnetic field.

The nonlinear interactions produce a flow of energy in wave number space that is predominantly from large to small scales, and although this can be described by interactions between neighboring wave number fluctuations, it is perhaps more easily visualized as compressive or shear-driven steepening. The resulting small-scale structures are sometimes localized and coherent and may be associated with the intermittency of solar wind turbulence. As indicated schematically in Figure 1, the spectrum of fluctuations can be divided into three ranges: the largest, “energy containing” scales that provide the reservoir tapped by the turbulent cascade; the intermediate “inertial range,” characterized by power-law spectra, where the nonlinear, inertial term in the equations of motion dominates over the dissipation; and the small-scale “dissipation range” in which the fluctuations are converted to thermal energy, which can lead to significant heating of the wind (and possibly also the solar corona). The evolving fluctuations may also help to accelerate the wind.

The next two sections provide overviews of the observations and theories of solar wind turbulence. We then deal with specific issues of present study, including the origin of the fluctuations near the Sun, and the relative roles of expansion, shear, and compression. We also deal briefly with the problem of the dissipation of the turbulent energy, and in this context discuss the issues that must be resolved to determine the role of turbulence in coronal heating and solar wind acceleration. The final section gives a brief picture of where we stand. The references are intended to give the reader a sufficient number of points of contact to trace the history and details of any particular area.

2. OVERVIEW OF OBSERVATIONS

2.1 *Early Observations*

From the earliest observations it was clear that all solar wind quantities were varying in time with changes in velocity, density, magnetic field, and temperature (see Figures 2 and 3 to be discussed further below). It was quickly realized that these fluctuations could be described with considerable success using the formalism of magnetohydrodynamic (MHD) waves. Both propagating MHD modes (Coleman 1966), predominantly the shear Alfvén mode (Belcher & Davis 1971, Unti & Neugebauer 1968), and convected structures (Burlaga & Ogilvie 1970) were identified. These observations confirmed Barnes' (1966) conclusion that kinetic effects would damp the magnetoacoustic modes. A striking feature of the observations was that the Alfvén waves were nearly always propagating outward from the Sun.

Coleman (1968) noted the similarity of the spectral slopes of power spectra of the magnetic fluctuations to those of velocity fluctuations predicted for isotropic magnetofluid turbulence (Kraichnan 1965); similar spectral behavior is seen in isotropic, homogeneous fluid turbulence (Kolmogoroff 1941). Motivated by these observations, Coleman suggested that the solar wind was a turbulent and dynamically evolving medium driven by stream-shear instabilities. He argued further that turbulent dissipation at high wave numbers could account for the anomalously high proton temperatures observed in the solar wind at 1 AU. This picture was subject to several criticisms: First, Belcher & Davis (1971) argued that it was difficult to reconcile turbulent generation by stream-shear with the observed outward propagation of the Alfvén waves. Second, in an incompressible and dissipationless magnetofluid, pure Alfvén waves are exact solutions of the MHD equations, and therefore no spectral evolution should occur. Furthermore, Parker (1964) argued that the mean magnetic field of the solar wind would suppress the shear-driven Kelvin-Helmholtz instability so that the high-speed streams could not generate a turbulent cascade. Bavassano et al (1978) argued that, even if excited, shear instabilities could not produce fluctuations on the large scales observed. To the extent that the turbulence viewpoint espoused by Coleman was rejected, the major source of interplanetary fluctuations then had to lie below the Alfvénic critical point in the solar corona as Belcher & Davis had suggested. Subsequent analysis of the role of the Kelvin-Helmholtz instability in the solar wind (Korzhov et al 1984) showed that Parker's analysis, because it ignored oblique wave vectors, was too pessimistic (see also Southwood 1968 and Miura & Pritchett 1982). In addition, it was realized that although the Alfvénic correlation in the solar wind was often very high, it rarely exceeded $\approx 90\%$, which is insufficient to suppress rapid nonlinear evolution (Matthaeus et al 1984).

2.2 *Waves vs Turbulence: More Recent Observations and a Proposed Resolution*

The observation of the variation of the plasma parameters with heliocentric distance is essential for understanding the origin and the forces driving the evolution of interplanetary fluctuations. Over the past three decades the launch of several spacecraft has made such studies possible. The excellent particle and fields experiments on the *Voyager* and *Helios* spacecraft, in particular, have permitted studies spanning heliocentric distances from 0.3 to beyond 30 AU.

Matthaeus & Goldstein (1982a) began a systematic study of the extent to which the turbulence model of the solar wind was consistent with observations. Their goal was to understand both the magnetic and velocity spectra and how these spectra related to macroscopic structure. Because compressive effects in the inertial range appeared relatively unimportant, they initially used incompressible, single-fluid MHD theory. Their analysis emphasized the important role of quadratic, integral invariants of nondissipative, incompressible, single-fluid MHD. From the spectra of the invariants one can learn much about the state and dynamics of the solar wind. In the absence of a mean magnetic field the most important quadratic invariants are the energy (per unit mass)

$$E = \frac{1}{2} \int d^3x (v^2 + b^2), \quad (1)$$

the cross helicity

$$H_c = \frac{1}{2} \int d^3x \mathbf{v} \cdot \mathbf{b}, \quad (2)$$

and the magnetic helicity

$$H_m = \int d^3x \mathbf{A} \cdot \mathbf{B} \quad (3)$$

(Woltjer 1958, Frisch et al 1975), where \mathbf{A} is the magnetic vector potential defined so that $\mathbf{B} = \nabla \times \mathbf{A}$, \mathbf{v} is the velocity, and \mathbf{b} is the magnetic field in Alfvén speed units, $\mathbf{B}/(4\pi\rho)^{1/2}$. When a mean field is present, the magnetic helicity is modified (Matthaeus & Goldstein 1982a). Of particular use in analysis and interpretation of solar wind data are the normalized measure of the reduced cross helicity, $\sigma_c \equiv 2H'_c/E'$, and its spectrum, $\sigma_c(f) \equiv 2H'_c(f)/E'(f)$, where the term “reduced” refers to integrating the spectral tensor over the two directions transverse to the direction of the solar wind velocity so that the spectra are functions only of wave number parallel to the solar wind velocity \mathbf{V}_{SW} . In this paper we define the cross helicity so that positive values always indicate outward propagation from the Sun, regardless of the direction of the mean magnetic field. Matthaeus et al (1982) first showed how to determine the magnetic helicity and its reduced spectrum from single-point measurements of the magnetic field.

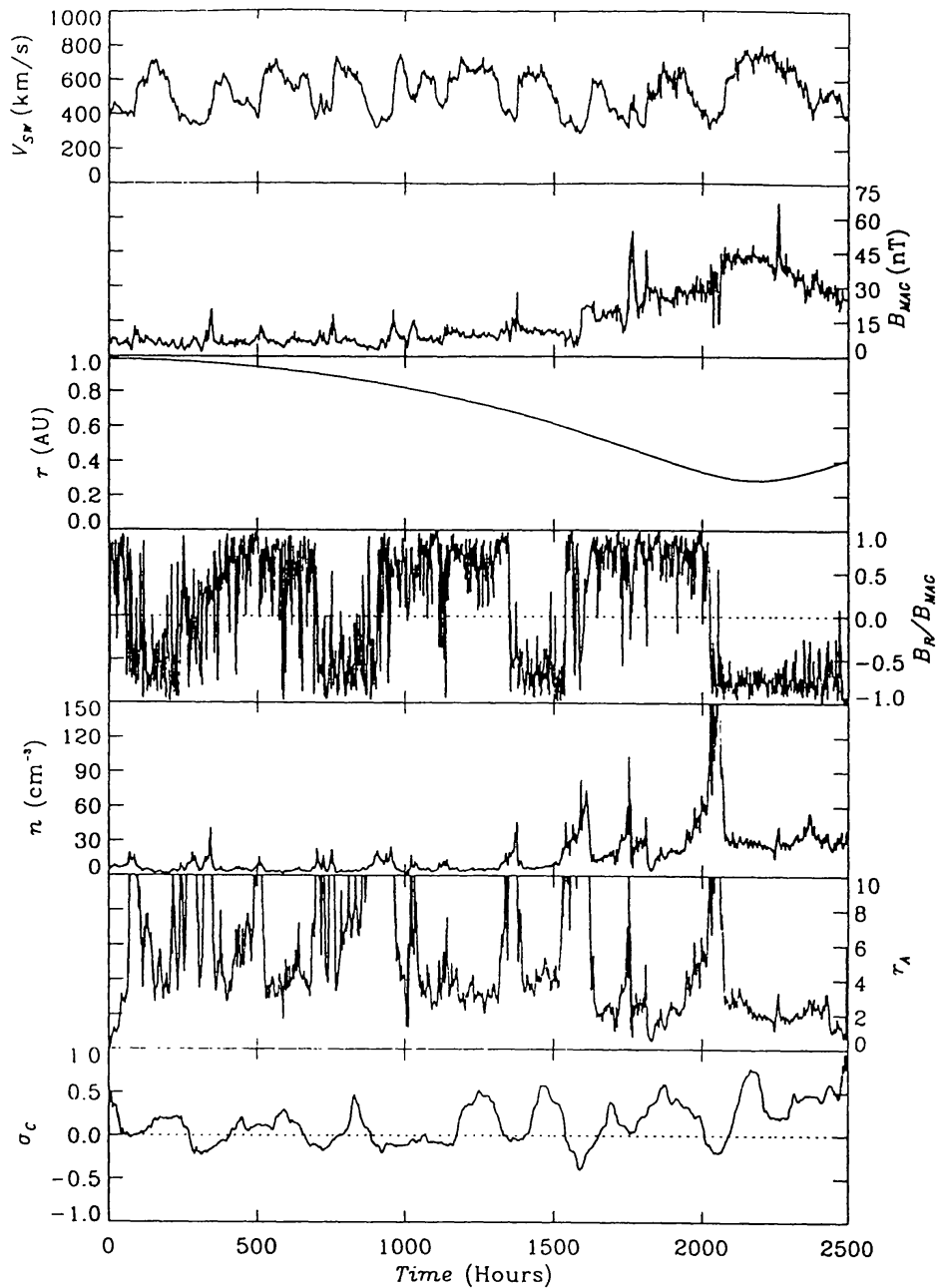


Figure 2a Large-scale features of about 100 days of hour-averaged data from the primary mission of *Helios 2* (early 1976). From top to bottom the panels are: the speed of the solar wind, showing recurrent high-speed streams; the magnitude of the magnetic field; the distance of the spacecraft from the Sun; the radial component of the magnetic field divided by the field strength, showing how the relative fluctuations increase with increasing distance; the density of the wind; the Alfvén ratio of kinetic to magnetic energy at a 10-day scale, showing the dominance of the radial velocity changes; and the normalized cross helicity at the 4-day scale.

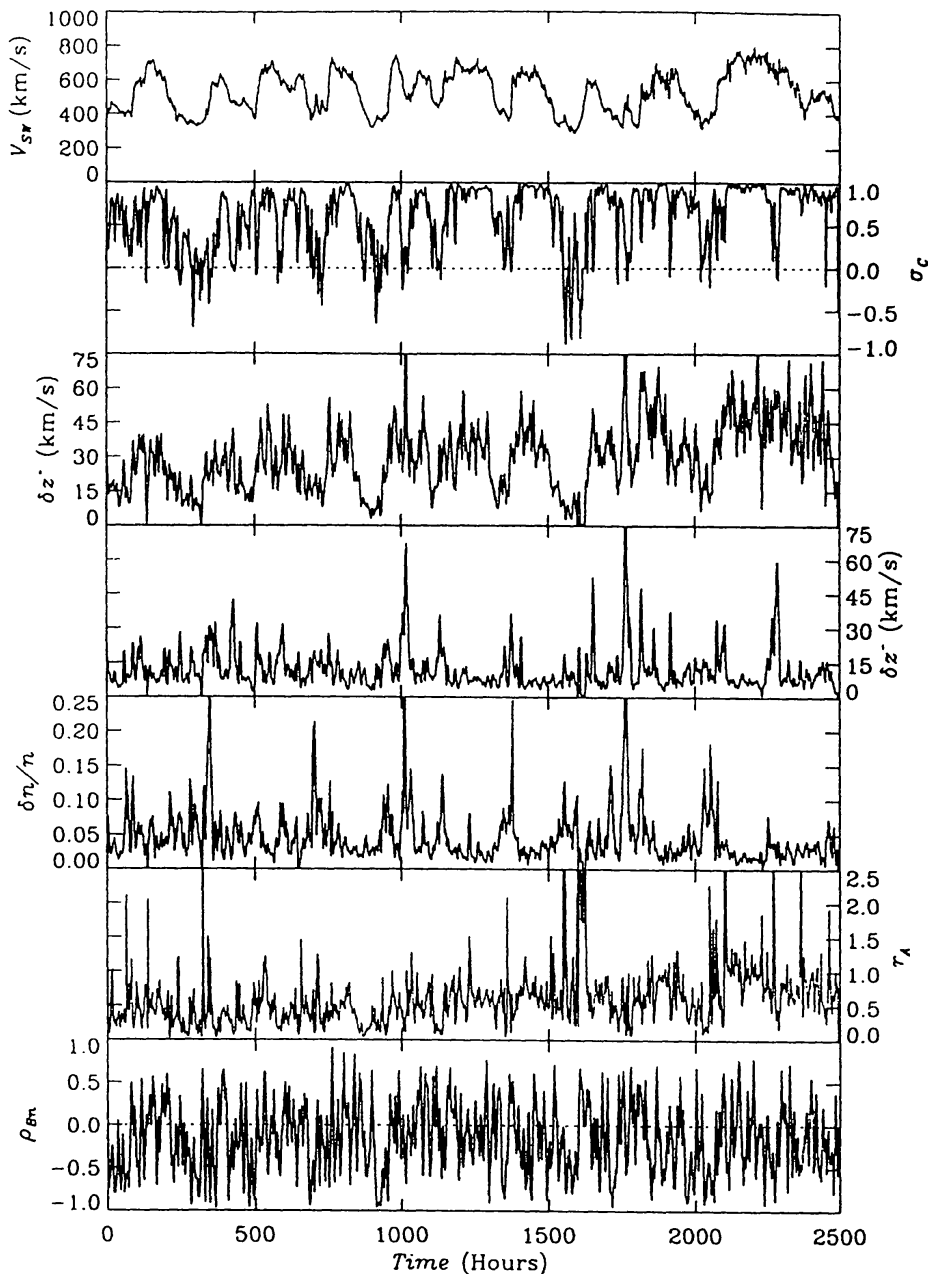


Figure 2b Small-scale features constructed from the same *Helios* data set. All fluctuating quantities are at the 3-hour scale, smoothed with a 7-hour window. From top to bottom: the speed of the solar wind (repeated for clarity from Figure 2a); the normalized cross helicity; the (declining) amplitude of the z^+ fluctuations; the (relatively constant) amplitude of the z^- fluctuations; the relative density fluctuations; the Alfvén ratio; and the correlation between density and magnetic field strength.

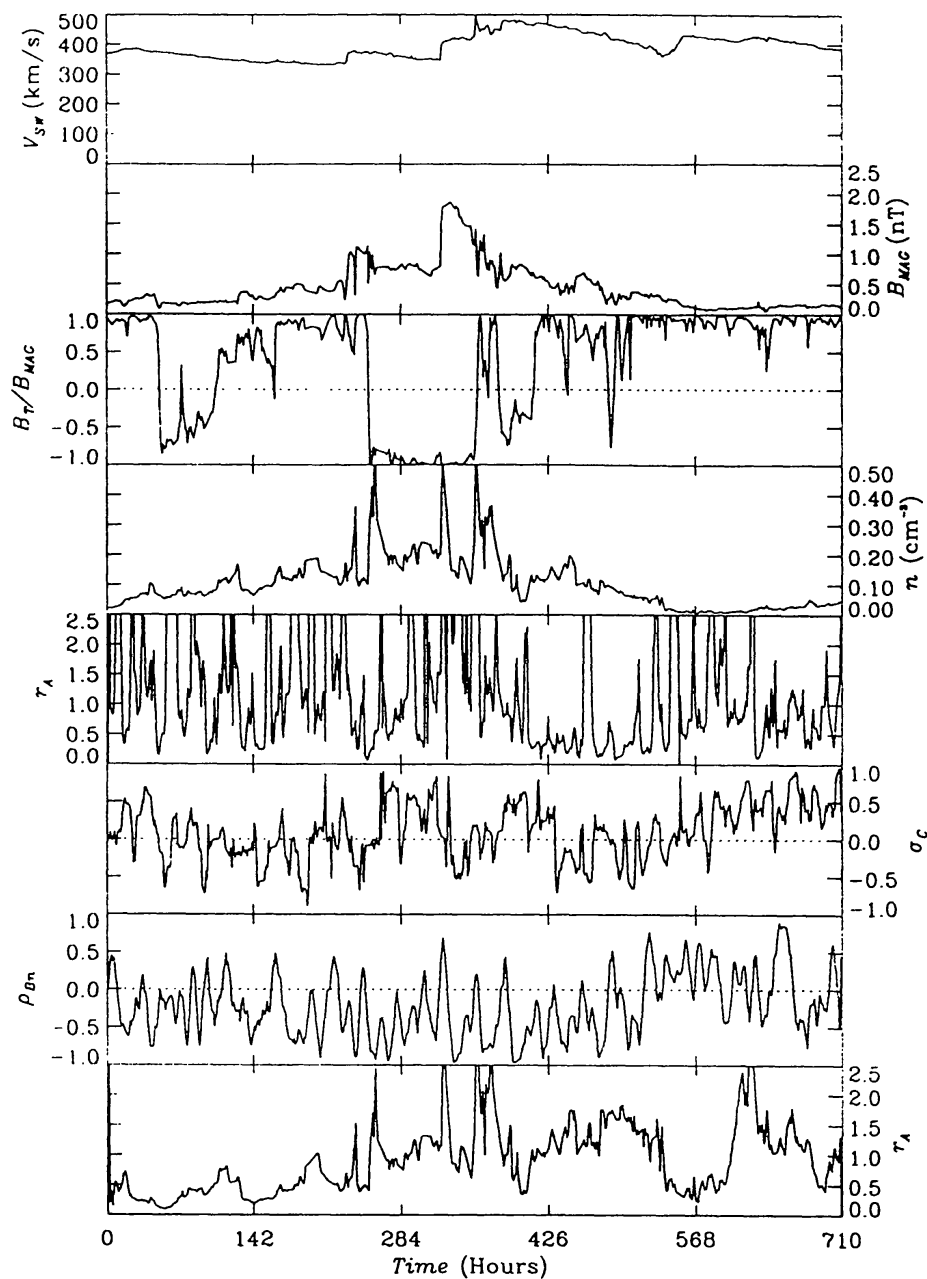


Figure 3 Hour-averaged *Voyager 1* data gathered near 8 AU in mid-1980, along with various derived quantities. From top to bottom: the solar wind speed; the magnitude of the magnetic field; the tangential component of the magnetic field compared to the field magnitude; the density, showing large compressions and a rarefaction toward the end of the interval (see also B_{mag}); the Alfvén ratio at the 3-hour scale, smoothed with a 7-hour window; the normalized cross helicity at the 3-hour scale, smoothed with a 7-hour window; the correlation between magnetic field and density at the 3-hour scale, smoothed with a 7-hour window; and the Alfvén ratio at the 10-day scale, showing the loss of stream dominance in the outer heliosphere.

From a single spacecraft, however, it is not possible to obtain a full three-dimensional spectrum of the invariants (Matthaeus & Goldstein 1982b); this therefore limits analyses to reduced spectra (Batchelor 1970).

The power spectra of magnetic fluctuations that Coleman constructed were power laws over a substantial range of scales with spectral index α between -1 and -2 . A value of $\alpha = -1$ over all wave numbers would imply infinite energy content; conversely, $\alpha = -2$ is characteristic of a medium dominated by discontinuities. Whereas fully developed homogeneous and isotropic fluid turbulence was known to have a value of $\alpha = -5/3$ (Kolmogoroff 1941, Grant et al 1962), Kraichnan's (1965) generalization to MHD suggested a value of $\alpha = -3/2$. Matthaeus et al (1982) showed that often $\alpha = -1.7 \pm 0.1$. The sample power spectrum constructed from *Mariner 10* magnetometer data from March 20, 1974, plotted in Figure 4, also has $\alpha \approx -5/3$. [Many subsequent studies have found similar results; see, for example, Marsch (1991).] Note that this spectrum shows a break to a steeper dissipation range at about 0.8 Hz, which indicates the presence of proton cyclotron damping.

The (reduced) power spectrum of the cross helicity (Matthaeus & Goldstein 1982a) generally indicated propagation of Alfvénic fluctuations outward from

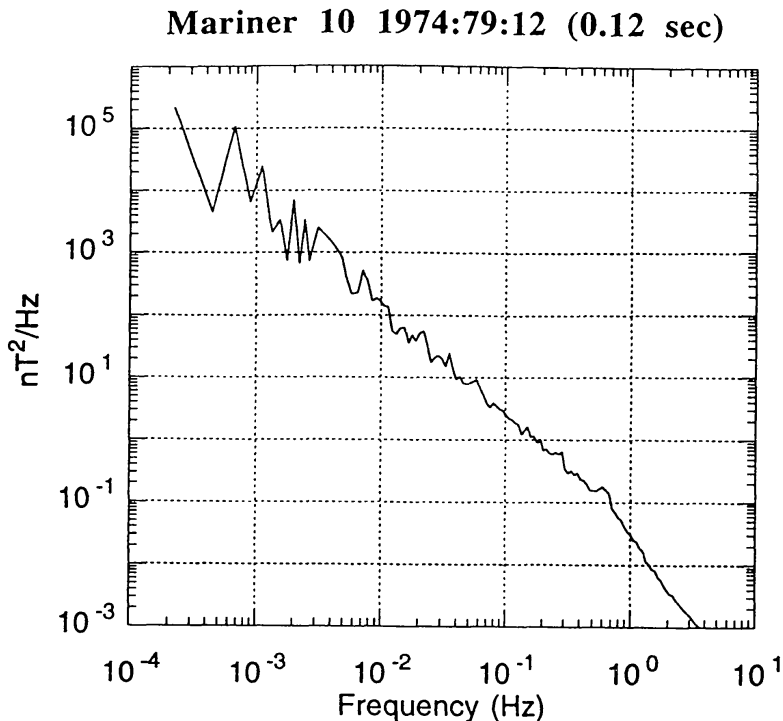


Figure 4 The trace of the power spectral matrix of the magnetic field fluctuations from a 74-minute interval of 0.12-second average *Mariner 10* magnetometer data obtained on March 20, 1974. Note that the inertial range has a spectral slope very close to $-5/3$, and a clearly defined dissipation range is apparent at the highest frequencies. This time series is too short to see the energy-containing scales.

the Sun, consistent with the Belcher & Davis (1971) result, but “mixed” cross helicity periods could be found beyond 1 AU. In contrast, the spectrum of the reduced magnetic helicity, which was also a power law with index $\alpha \approx -7/3$, indicated random fluctuations between positive and negative values throughout the inertial range of the spectrum. Recently, Goldstein et al (1994) found that only the dissipation range showed any tendency of a systematic value of helicity, an effect also consistent with cyclotron damping.

Kraichnan (1965) had predicted that the magnetic and kinetic energy (per unit wave number) should be equal, on average, in the inertial range of magnetofluid turbulence. He argued that because Alfvénic solutions ($\delta \mathbf{v} = \pm \delta \mathbf{b}$) of arbitrary amplitude are exact solutions of the dissipationless incompressible MHD equations, a perturbation of $\delta \mathbf{v} \neq \mathbf{0}$ (with $\delta \mathbf{b} = \mathbf{0}$) can be thought of as an initial condition for two Alfvén wave packets with magnetic fluctuations $+\delta \mathbf{b}$ and $-\delta \mathbf{b}$, respectively. Because the packets will propagate away from each other (Moffatt 1978, Parker 1979) with speeds $B_0/(4\pi\rho)^{1/2}$, where $\mathbf{B} = \mathbf{B}_0 + \delta \mathbf{B}$ (with $\mathbf{B}_0 = \langle \mathbf{B} \rangle$ as the time-averaged field), approximate equipartition should result. A measure of this is the “Alfvén ratio” $r_A = E_V(k)/E_B(k)$, where $E_V(k)$ and $E_B(k)$ are the reduced spectra of the kinetic energy and magnetic energy, respectively. Although some evidence for equipartition was reported in two-dimensional simulations (Fyfe & Montgomery 1976), the data plotted in Figures 2b and 3 illustrate that in the solar wind the average values of r_A in the inertial range of the spectrum are between 0.4 and 1.0 (Matthaeus & Goldstein 1982a; Roberts 1992; Roberts et al 1987a,b, 1989, 1990, 1992). At the ~ 10 day scale, r_A is dominated by large fluctuations in the radial component of the solar wind velocity (Figure 2a), even within streams, while at the smaller scales (Figure 2b) at ~ 0.3 AU, $r_A \approx 1$, decreasing to ~ 0.5 by 1 AU. In the outer heliosphere, as seen by *Voyager 1* at 8 AU (Figure 3), despite large variations and brief spikes (some of which are associated with data gaps), r_A still has a most probable value ~ 0.5 .

We have used “Alfvénic” to refer to the degree to which the interplanetary fluctuations resembled outward-propagating Alfvén waves, i.e. a medium with high cross helicity. This is somewhat confusing because a fluid in which Alfvén waves propagate both parallel and antiparallel to a mean magnetic field would have a small cross helicity and would not be “Alfvénic” in the sense used above. To better describe the behavior of inward- and outward-propagating fluctuations, one often uses the Elsässer variables (Elsässer 1950, 1956) defined by $\mathbf{z}^\pm = \delta \mathbf{v} \pm \delta \mathbf{b}$, where \mathbf{z}^+ and \mathbf{z}^- refer to waves propagating “outward” and “inward” with respect to \mathbf{B}_0 . Elsässer variables are most useful for describing incompressible MHD because in the ideal limit either $\mathbf{z}^+ = \mathbf{0}$ or $\mathbf{z}^- = \mathbf{0}$ are exact solutions. Dobrowolny et al (1980a,b) used Elsässer variables to argue that solar wind fluctuations should have increasing cross helicity if they are predominantly of one sign initially (“dynamic alignment”). Later, Goldstein et al (1986) showed how the variables could be used to correct a systematic emphasis

toward outward propagation in the interpretation of solar wind data in low Mach number flows. The Elsässer formalism was generalized for compressible MHD by Marsch & Mangeney (1987) and the variables have proven useful in trying to ascertain the relative roles of velocity shear and compressibility in driving interplanetary turbulence (Marsch 1991, Roberts 1992, Roberts & Goldstein 1991).

An example of the general behavior and evolution of the fluctuations in z^{\pm} is shown in Figure 2*b*. The quantities δz^+ and δz^- are measures of the relative behavior of the Elsässer variables obtained by subtracting 3-hour averages of the vector components of the z^{\pm} from the total vectors, computing the magnitude of the resulting variations, and then plotting the 7-hour average of the result. Note that in the inner heliosphere z^+ is large and decreases as one approaches 1 AU. In contrast, z^- is relatively small and constant from 0.3 to 1 AU. The spectra of z^+ also evolve rapidly in the inner heliosphere, approaching z^- by 1 AU. In highly Alfvénic regions near the Sun, z^+ (“outward”) has a flat spectrum at low frequencies and a spectral index $\alpha \approx -5/3$ at high frequencies, while z^- shows nearly the reverse behavior (Figure 5). This tendency can be qualitatively understood in terms of the “minority species effect” developed by Matthaeus et al (1984) to explain dynamic alignment and is also predicted in closure calculations (e.g. Grappin et al 1983). Farther out, the spectra of both z^+ and z^- tend to be nearly parallel except at low frequencies where they merge (Figure 6).

One of the puzzles of MHD turbulence is trying to understand the observed power spectrum of the density. Whether computed from in situ solar wind observations (Goldstein & Siscoe 1972) or from radio scintillation techniques (Armstrong et al 1981, 1990; Scott et al 1983; Woo & Schwenn 1991; Woo & Armstrong 1979; Higdon 1984), the power spectrum of density fluctuations has the same $\alpha = -5/3$ spectral slope as do components of the magnetic field and velocity, although the spectra of density, temperature, z^- , and magnetic field magnitude all tend to flatten at high wave numbers in some regions of the inner heliosphere.

Implicit in our discussion is that construction of a power spectrum from time series of solar wind magnetic field or plasma data is valid. Matthaeus & Goldstein (1982*b*) tested this assumption and showed that the time series of the interplanetary magnetic field ranging from days to years did indeed satisfy the conditions of “weak” stationarity when the effects of solar rotation were included. Using their technique for selecting stationary intervals, Matthaeus et al (1986) constructed an interplanetary field ensemble from data collected near 1 AU and used the ensemble to determine various statistical properties of the interplanetary magnetic field, including the correlation time and length of the magnetic field ($\approx 4.9 \times 10^{11}$ cm), the average direction of the field, etc, along with the variances of those quantities.

The evolution of the cross helicity is arguably the most significant diagnostic of turbulent behavior in a magnetofluid. Simulations have shown that the long-

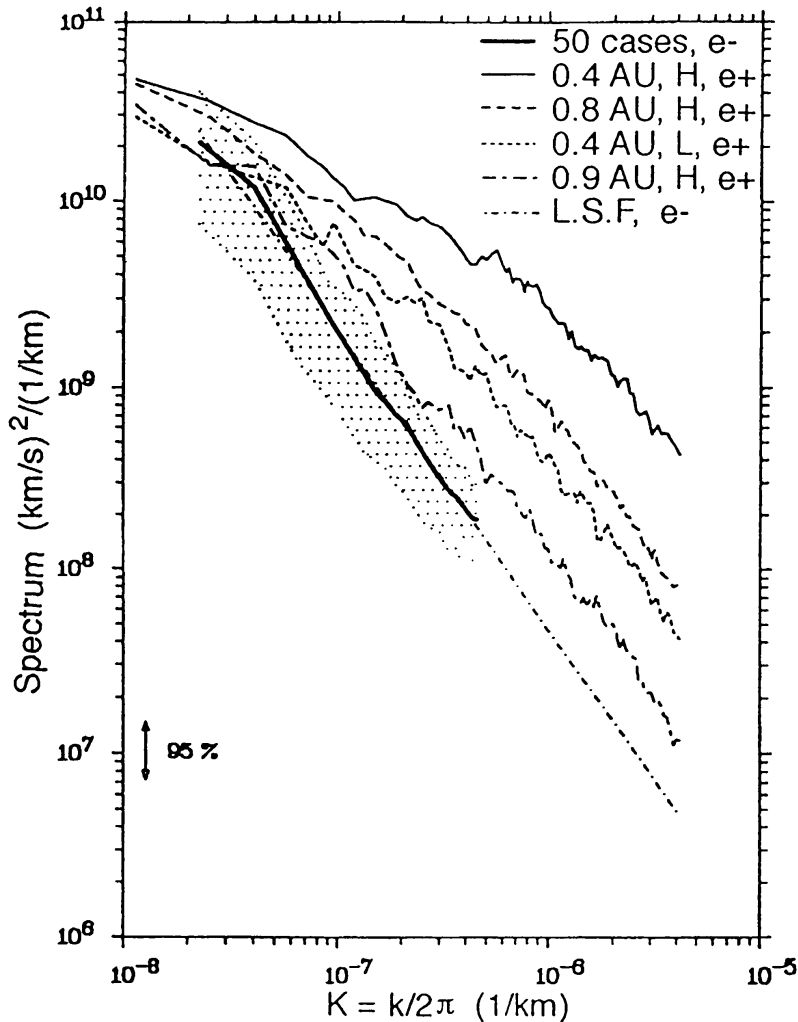


Figure 5 The Elsässer variable spectra for high-speed (solid line) and low-speed (dotted line) streams from the *Helios* data described in Figure 2. (Adapted from Marsch & Tu 1990a.)

time behavior of the cross helicity depends sensitively on initial conditions (see, for example, Ting et al 1986, Ghosh et al 1988, Ghosh & Matthaeus 1990, Roberts et al 1992); thus, by comparing changes in the heliospheric behavior of the cross helicity with simulations and theory, one hopes to discover the physical mechanisms that control the excitation and evolution of turbulence in the solar wind. Investigations were made with magnetometer and plasma data by Bruno et al (1985), who used only low-frequency *Helios* data, and by Roberts et al (1987a,b), who also included *Voyager* data as well. Both studies demonstrated that outward-propagating Alfvén waves ($\sigma_c > 0$) become less predominant with increasing heliocentric distance. This is illustrated for the large-scale fluctuations in Figure 2a and for the smaller-scale fluctuations in Figure 2b (note also the low values in “structured” regions). At neither scale is this decrease in Alfvénicity accompanied by any significant increase in negative values of σ_c , as might be expected if sufficient time had elapsed for

the faster evolving small amount of inward-propagating fluctuations (“minority species” effect) to become important (Matthaeus et al 1984, Grappin et al 1983). Similarly, the highly Alfvénic character of many intervals near 0.3 AU down to scales longer than the transit time to the spacecraft indicate that no reservoir of large-scale inward-propagating fluctuations is present, as was suggested by Matthaeus et al (1984). Roberts et al (1987a,b) concluded from this analysis that the solar atmosphere had to be the main source of the outward wave flux at 0.3 AU, as had been conjectured initially by Belcher & Davis (1971).

The same data set, however, provides evidence that regions of strong velocity shear are characterized by rapid decreases in σ_c (see also Bavassano & Bruno 1989). This is especially clear in Figure 2*b*, where comparison of the top two panels (V_{SW} and σ_c) shows that rapid reductions of σ_c are associated with sharp changes in V_{SW} . Regions of nearly pure outward-propagating Alfvén waves are present when the velocity gradients are small; these include, but are not restricted to, the trailing edges of high-speed streams. Similar behavior is present in the outer heliosphere as can be seen in Figure 3: Near the end of the interval, in a rarefaction region with small velocity gradients and that has been relatively undisturbed in its journey to 8 AU (Whang & Burlaga 1985), σ_c is

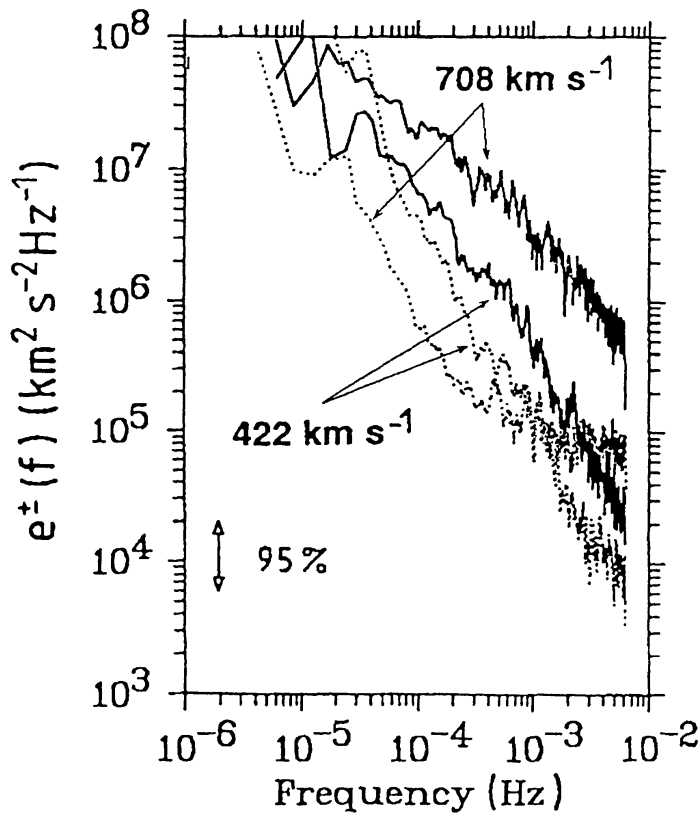


Figure 6 The evolution of the Elsässer variable spectrum of z^+ from 0.4 to 1 AU plotted along with a least-squares fit to 50 z^- spectra (bottom dash-dot line) and the spectral range of the 50 spectra indicated by the dappled band. (From Tu & Marsch 1990a.)

still large and positive. Roberts et al (1987a,b) also argued that the degree of Alfvénicity was nearly independent of the degree of compression in the wind; it is only slightly less in compression regions than in stream rarefaction regions (cf Figure 2), although the relative density fluctuations do show correlation with z^- fluctuations (Figure 2b).

Pressure balance structures are another feature of the solar wind that vary markedly with heliocentric distance. The percentage of the time that the correlation between $|\mathbf{B}|$ and $\delta\rho$ is less than -0.8 increases with distance (Figures 2 and 3). This is the strongest indicator of evolution and indicates that the compressive component of the fluctuations becomes dominated by pressure balance structures in the outer heliosphere (Roberts 1990). Strong anticorrelations between $|\mathbf{B}|$ and $\delta\rho$ exist in the filamentary, structured regions in the inner heliosphere (Klein et al 1993a and Figure 2b). Anticorrelations of the same type as are expected in pressure balanced structures are a feature of nearly incompressible solutions to the MHD equations (Matthaeus et al 1991).

In the absence of any sources of heating, the solar wind temperature should decrease adiabatically due to the expansion of the wind. The details of the decrease in temperature with distance depend on the type of flow, but generally the decrease is slower than expected from adiabatic cooling alone (Freeman 1988, Freeman et al 1992, Lopez & Freeman 1982, Schwenn 1983), suggesting that heat is being added to the wind. If the polytropic index of the fluid is approximately $5/3$, the adiabatic temperature variation is $T(r) \propto r^{-4/3}$, which is too strong to be overcome by either turbulent or shock heating. The observed rate of decrease of temperature in the inner heliosphere ranges between -0.78 and -1.33 , with little difference seen in fast or slow streams (Marsch & Richter 1987). Gazis (1984) studied the temperature evolution in the outer heliosphere using *Voyager 1* data and found that various velocity streams had approximately similar temperature gradients, even though the faster ones were hotter. He concluded that $T \propto r^{-0.7}$ for all streams (see also Tu 1987). These studies suggest that additional heating sources must be present in the solar wind. Contributions from turbulent dissipation, shock heating, and interstellar pickup ions all vary with distance, and their relative importance has not yet been determined.

A comprehensive account of solar wind phenomenology should also explain the observed tendency for the direction of minimum variance of magnetic field fluctuations to lie along the direction of the mean magnetic field. This property of the interplanetary field was first reported by Belcher & Davis (1971) using data obtained near 1 AU, and confirmed by Bavassano et al (1982) and Klein et al (1993b) for the inner heliosphere and by Klein et al (1991) and Parker (1980) for the outer heliosphere. As one moves outward in the heliosphere, fluctuations in velocity, which initially are more isotropic than the magnetic fluctuations, show little evolution with distance, while magnetic fluctuations become less anisotropic and by 2 AU have the same 3:1 anisotropy (the ratio

in power transverse to the minimum variance direction to that along it) as do the velocity fluctuations. However, although the minimum variance direction of the magnetic fluctuations lies along the average field direction, the minimum variance direction of the velocity fluctuations tends more toward the radial direction (Klein et al 1991). There has been considerable controversy about the interpretation of these results (Denskat & Burlaga 1977, Solodyna & Belcher 1976) because the observations are at variance with the predictions of WKB theory (Hollweg 1975, Völk & Alpers 1973).

Although we have known since the early work of Belcher & Davis (1971) that the solar wind fluctuations are not isotropic, the assumption of isotropy underlies most turbulence paradigms. There are two issues that need resolution: First, it is necessary to determine the degree of symmetry of solar wind fluctuations and to modify theoretical models accordingly. With single-point measurements it is not possible to specify the three-dimensional form of the spectral tensor of the magnetic or velocity fluctuations. In the absence of data, theoretical models of, for example, energetic particle propagation in the interplanetary medium have assumed various forms for the spectral tensor, including the “slab,” in which all nonzero spectral amplitudes are associated with wave vectors \mathbf{k} parallel to an ambient mean magnetic field; the isotropic model, in which all wave vectors with the same magnitude all have equal spectral amplitudes; and the quasi-two dimensional model, in which wave vectors are nearly perpendicular to the large-scale magnetic field \mathbf{B} while the magnetic fluctuations are orthogonal to both \mathbf{k} and \mathbf{B} .

In laboratory plasmas that contain a strong DC magnetic field, evidence exists for the presence of quasi-two dimensional turbulence (Robinson & Rusbridge 1971, Robinson et al 1968, Rusbridge 1969, Zweben et al 1979, Zweben & Taylor 1981). Those experiments motivated development of a theory of turbulence in the presence of a strong mean magnetic field (Montgomery 1982) based on the Strauss equations (Strauss 1976). The tendency of magnetic fluctuations to become highly anisotropic when a strong magnetic field is present has been confirmed in numerical simulations (Goldstein et al 1987a,b; Matthaeus & Lamkin 1985; Roberts et al 1992; Shebalin et al 1983; Oughton et al 1994).

Some techniques have been developed to search for anisotropies in solar wind data. Sari & Valley (1976) analyzed separately periods when the direction of the DC field was quasi-parallel and quasi-perpendicular to the solar wind velocity. Other studies using radio scintillation observations (Armstrong et al 1990, Woo & Armstrong 1979) indicate that density spectra near the Sun are highly anisotropic with the irregularities stretched out approximately along the radial direction. Matthaeus et al (1990) used long stationary data intervals, constructed an ensemble, and from that formed two-dimensional correlation functions using 5-min averages of 16 months of nearly continuous *ISEE 3* data. However, the data were too sparse to transform the correlation function into a power spectrum.

Nonetheless, they presented fairly strong evidence that the ensemble of data was neither “slab-like” Alfvén waves nor isotropic, but rather consisted of two populations: fluctuations with large correlation lengths transverse to $\bar{\mathbf{B}}$ (Alfvénic) and fluctuations with large correlation lengths parallel to $\bar{\mathbf{B}}$ (quasi-two dimensional). ($\bar{\mathbf{B}}$ is the direction of the average magnetic field in the data interval used for the correlation calculation.) At small separations, $r \leq 5 \times 10^{10}$ cm, Alfvénic- or slab-symmetry appeared dominant, whereas contributions from a quasi-two dimensional component became noticeable for $r \geq 15 \times 10^{10}$ cm. The analysis suggests that the solar wind contains a population of Alfvénic fluctuations, probably originating in the solar corona, along with a quasi-two dimensional component that could be evidence of turbulent evolution beyond the corona. Carbone et al (1995) have recently completed a similar study using a different approach, but arriving at somewhat similar conclusions.

If the solar wind really contains a strong quasi-two dimensional component, several long-standing puzzles would have immediate solutions. For example, pitch-angle scattering by resonant wave-particle interactions is suppressed in quasi-two dimensional turbulence and scattering mean free paths become long. The mean free paths of solar cosmic rays are known to be much longer than can be accounted for from standard quasi-linear theory using either isotropic or slab symmetry (see, for example, Kunow et al 1991). Bieber et al (1994) calculated cosmic ray mean free paths based on quasi-linear theory using a dynamic turbulence model and a mixture of quasi-two dimensional and slab magnetic fluctuations and found agreement with observed particle mean free paths. Furthermore, the direction of minimum variance of magnetic fluctuations in quasi-two dimensional turbulence will be parallel to \mathbf{B}_0 .

The evidence presented above shows that Belcher & Davis were correct in concluding that the high degree of Alfvénicity and outward propagation implied a source for the fluctuations that lay in the solar corona below the super-Alfvénic point. However, the strong evolution of the fluctuations with heliocentric distance and in the vicinity of large velocity shears showed that Coleman had correctly inferred that the free energy in stream-stream interactions would drive an in situ turbulent stirring of the medium that would determine the subsequent evolution of the fluctuations.

3. THEORETICAL AND SIMULATION MODELS OF TURBULENCE

3.1 *Applicability of MHD for Describing Solar Wind Phenomena*

Solutions of the MHD equations have proven invaluable in understanding many aspects of the turbulent evolution of fluctuations in the solar wind. In the following sections we discuss some of the problems tackled thus far using these

tools, including radial evolution of fluctuation amplitudes and temperature, the role played by velocity shear in driving the turbulence, and the role of compressibility and compressive structures. Although considerable progress has been made in understanding the evolution of the solar wind using incompressible MHD (Montgomery 1983), a complete description of solar wind evolution and dynamics must include compressive effects. Kinetic effects, while clearly important in the solar wind, will not concern us here, primarily because our present theoretical and computational capabilities are inadequate to describe the inertial scale or energy-containing scales of solar wind fluctuations using kinetic theory, but, secondarily, because the questions we are addressing require a more “coarse-grained” fluid approach.

3.2 MHD Equations

The MHD equations describe eight fields: the density ρ , velocity \mathbf{v} , temperature T , and magnetic field \mathbf{b} . In dimensionless units, the (compressible) MHD equations are continuity

$$\frac{\partial \rho}{\partial t} = -\nabla \cdot (\rho \mathbf{v}), \quad (4)$$

momentum

$$\frac{\partial \mathbf{v}}{\partial t} = -\mathbf{v} \cdot \nabla \mathbf{v} + \frac{1}{\rho} (\mathbf{j} \times \mathbf{B} - \nabla p + \nabla \cdot \underline{\tau}), \quad (5)$$

Maxwell's equations, neglecting the displacement current,

$$\begin{aligned} \frac{\partial \mathbf{B}}{\partial t} &= -\nabla \times \mathbf{E} \\ \mathbf{j} &= \nabla \times \mathbf{B} \end{aligned} \quad (6)$$

$$\nabla \cdot \mathbf{B} = 0,$$

together with Ohm's Law

$$\mathbf{E} = -\mathbf{v} \times \mathbf{B} + \eta \mathbf{j}, \quad (7)$$

and either a polytropic equation of the form $p = \rho^\gamma$ or an energy equation with the ideal gas law. In Equations (4–7), η is the resistivity and ν is the viscosity. The tensor $\underline{\tau} = \nu[\nabla \mathbf{v} + (\nabla \mathbf{v})^T] - \frac{2}{3}\nu(\nabla \cdot \mathbf{v})\mathbf{I}$ is the hydrodynamic viscous stress tensor, where \mathbf{I} is the unit tensor and ν is the dimensionless kinematic fluid viscosity. Anisotropies in the dissipation and the bulk viscosity are ignored. In the results discussed here, we used a polytropic closure and we do not consider energy equations further. In the incompressible limit ($\rho = \text{const.}$) Equations (4–7) become:

$$\begin{aligned} \frac{\partial \mathbf{v}}{\partial t} + \mathbf{v} \cdot \nabla \mathbf{v} &= \mathbf{b} \cdot \nabla \mathbf{b} - \frac{1}{2} \nabla b^2 + \nu \nabla^2 \mathbf{v} - \nabla p \\ \frac{\partial \mathbf{b}}{\partial t} + \mathbf{v} \cdot \nabla \mathbf{b} &= \mathbf{b} \cdot \nabla \mathbf{v} + \eta \nabla^2 \mathbf{b} \\ \nabla \cdot \mathbf{v} &= \nabla \cdot \mathbf{b} = 0. \end{aligned} \quad (8)$$

The unit of time is the “eddy-turnover time” for a unit velocity field of unit length scale.

3.3 *MHD Turbulence: Definitions and Comparison to Other Viewpoints*

The central issue separating the “wave” and “turbulence” viewpoints is the role of nonlinear interactions. The linearized, compressible MHD equations yield three traveling modes (Barnes 1979): the slow or acoustic mode; the Alfvén, intermediate, or shear Alfvén mode; and the fast or “compressional Alfvén” mode. In addition, the equations admit solutions for nonpropagating structures in which the magnetic and thermal pressures balance. The slow and fast modes are strongly damped except for some special directions of propagation of the fast mode (Barnes 1966); this is presumably what leads to the dominance of the Alfvén mode in the observed fluctuations.

In fluid turbulence, neighboring wave numbers couple strongly, leading to a conservative transport of energy in wave-number space that is halted by the formation and dissipation of very small structures (see Figure 1). The Reynolds number, $Re = UL/\nu$, measures the relative strength of the nonlinear and viscous stresses at the scale L of the correlation length of the fluctuations. As Re increases, the scale for dissipation decreases such that the rate of energy cascade through the inertial range, on average, equals the small-scale dissipation rate in steady state. Assuming that the cascade rate is independent of Re leads to the well-verified Kolmogoroff spectrum (Grant et al 1962). In particular, if the dissipation rate ϵ equals the cascade rate and depends only on the energy per wave number E_k and the wave number $k = |\mathbf{k}|$, then for an isotropic shell in the k -space dimensional analysis gives

$$E_k = C_K \epsilon^{2/3} k^{-5/3}, \quad (9)$$

where C_K is a universal “Kolmogoroff constant.”

The situation for a magnetized plasma is more complex than the fluid case because both the mean magnetic field and the cross helicity strongly affect the cascade rate (Grappin et al 1983, Matthaeus & Zhou 1989, Zhou & Matthaeus 1990a, Tu & Marsch 1990b). Kraichnan (1965) argued that a strong background magnetic field would lower the interaction time of the eddies to $\tau_A = 1/(kV_A)$. If τ_{NL} denotes the characteristic time taken for the nonlinear term to change the velocity substantially in the absence of magnetic fields, it would take τ_{NL}/τ_A *coherent* interactions, each of time τ_A , to produce the same change as τ_{NL} without the field, but if we suppose that each interaction is independent of the others it will take $(\tau_{NL}/\tau_A)^2$ interactions. This means the time for spectral transfer will be increased from τ_{NL} to $\tau_s \equiv (\tau_A)(\tau_{NL}/\tau_A)^2 = \tau_{NL}^2/\tau_A$. The steady state spectrum that results is proportional to $k^{-3/2}$. A more general case can be obtained by including a nonlinear time for each of z^\pm , and by replacing τ_A in the above argument with τ_3 , the triple decorrelation time arrived at by

taking the sum of the rates for nonlinear and Alfvénic processes (Kraichnan 1965, Matthaeus & Zhou 1989, Pouquet et al 1976). Then

$$(\tau_3^\pm)^{-1} = \tau_A^{-1} + (\tau_{NL}^\pm)^{-1} \quad (10)$$

and

$$\tau_s = \tau_{NL}^2 / \tau_3. \quad (11)$$

Now $\tau_{NL}^\pm = 1/(k^3 E^\pm)^{1/2}$ because it is z^+ that convects z^- and vice versa. Combining the above gives the rates of spectral transfer

$$\frac{1}{\tau_s^\pm} = \frac{k^2 E^\mp}{V_A + (k E^\mp)^{1/2}} \quad (12)$$

and dissipation rates

$$\epsilon^\pm \equiv \frac{(z_k^\pm)^2}{\tau_s^\pm} = \frac{k^3 E_k^+ E_k^-}{V_A + (k E^\mp)^{1/2}}. \quad (13)$$

Cascades are now slowed by either a strong external field or a high cross helicity, and the cascade rates of z^+ and z^- are no longer equal.

In the solar wind the spectral evolution with distance necessitates modification of these steady state arguments. The simplest model for near steady state cases, initially applied by Tu et al (1984) and Tu (1988), is one in which ϵ gives the local flux F_k out of a shell of radius k in wave vector space. Then with $F_k = \epsilon(k)$,

$$\left(\frac{\partial E_k}{\partial t} \right)_{NL} = - \frac{\partial F_k}{\partial k}. \quad (14)$$

A more complex but in some ways preferable approximation is to treat the flow of energy in k -space as diffusive (Zhou & Matthaeus 1990a, Leith 1967, Oughton 1993).

3.4 *Simulations: Overview of Spectral Codes and Algorithms*

Numerical algorithms for studying turbulence must be designed to describe accurately the steeply falling power spectra characteristic of fully developed MHD turbulence and its relationship to solar wind evolution and structure. However, modeling the three or more decades of scale sizes in the inertial range of solar wind fluctuations is not yet possible in three dimensions—a little more than two decades is the present practical limit. One advantage of spectral algorithms is that they do not contain numerical dissipation; one disadvantage, however, is that they are generally limited to highly idealized boundary conditions. Although most of the results discussed below employed up to 256^2 Fourier modes, this is insufficient to resolve a well-defined inertial range, which requires resolutions of at least 512^2 together with hyperresistivity

and hyperviscosity (Passot & Pouquet 1988, Biskamp & Welter 1989, Verma 1994).

Additional simplifications include ignoring the influence of the substantial ($\approx 5\%$ by number) presence of alpha particles (and other minor ions) and disregarding any anisotropies in pressure and temperature. Using the incompressible equations does, however, have theoretical motivation (Matthaeus & Brown 1988; Matthaeus et al 1991; Montgomery et al 1987; Zank & Matthaeus 1990, 1992a,b; Zank et al 1990). Results from solutions of the incompressible MHD equations provide a basis for comparison both with results of compressive simulations (Roberts et al 1991, 1992) and incompressive multi-length-scale MHD turbulence modeling theories (Marsch & Tu 1989; Zhou & Matthaeus 1989, 1990a,b,c; Zhou et al 1990). MHD turbulence simulations have begun to include aspects of the effects of the expansion of the medium with increasing heliocentric distance (Grappin et al 1993a,b). Two-and-a-half-dimensional simulations (in which all three components of the fluctuating magnetic and velocity fields are included), or three-dimensional simulations, are necessary for studying the evolution of the magnetic helicity; Stribling & Matthaeus (1995), Stribling et al (1995a,b), and Ghosh et al (1994) have reported on such studies.

3.5 *Turbulence Modeling*

The solar wind, expanding outward from the Sun and permeated by fast and slow streams as well as solar transients, is an intrinsically inhomogeneous medium. WKB theory, generally valid for weak inhomogeneities and small amplitudes (Hollweg 1973a,b, 1974), fails to predict the presence of any inward-propagating fluctuations and the field-aligned direction of minimum variance of magnetic fluctuations, and it predicts that $r_A \approx 1$, while $r_A \approx 1/2$ is more common. Heinemann & Olbert (1980) generalized WKB to include non-WKB (finite wavelength) effects. The basic structure of their equations was

$$\frac{\partial f^\pm}{\partial t} + (U \pm V_A) \frac{\partial f^\pm}{\partial s} = f^\mp (U \pm V_A) \frac{d\psi}{ds}, \quad (15)$$

where spherical geometry and incompressive fluctuations were assumed. The variable f^\pm is z^\pm normalized to take into account the WKB variation in amplitudes, s is arc length along a field line, and ψ is a normalized solar wind density. The terms on the right-hand side generalize WKB to include gradients in density and “drive” the generation of inward (outward) waves from outward (inward) waves—a process described as “reflection,” “scattering,” or “mixing.” When the wave numbers along the direction of the magnetic field are high, these non-WKB terms have rapidly changing phases with respect to the driven terms so that inward and outward waves pass through each other without resonant interaction or coupling. Thus, for small-scale parallel-propagating waves, an initially outward Alfvénic disturbance remains Alfvénic;

its amplitude decays following WKB ($\delta B \propto r^{-3/2}$) and velocity fluctuations remain equipartitioned and aligned with the magnetic fluctuations. Consequently, this extension of WKB (see also Hollweg 1990) cannot cure the deficiencies of WKB.

Subsequently, a variety of models have been developed in an attempt to improve this situation. The ultimate goal is to unify the wave propagation and turbulence evolution paradigms, and a number of initial efforts have been made in this direction (Marsch & Tu 1989, 1990a,b; Tu 1988; Tu & Marsch 1990a,b, 1992; Tu et al 1984; Zhou & Matthaeus 1989, 1990a,b,c). One begins with the ideal single-fluid MHD equations and assumes that the average large-scale spatial variations, which are $\sim R$ the local heliocentric distance, are well separated from the plasma fluctuations, which have a correlation length $\lesssim 1/10 R$. One then writes the velocity, magnetic field, density, and pressure as ensemble-averaged slowly varying quantities plus rapidly varying small-scale perturbations. The original MHD equations are ensemble averaged and the results are subtracted from the original equations to yield a set of equations for the fluctuating quantities. From these, one derives equations for the evolution of a variety of correlation functions, which can be further simplified by treating the small-scale quantities as incompressible so that $\delta\rho = \nabla \cdot \mathbf{v} = 0$. Although in principle the ensemble-averaged magnetic field, solar wind velocity, and density can be influenced by the fluctuating fields, one assumes that they are known: $\langle \mathbf{V} \rangle = \text{constant}$, $\rho \sim 1/R^2$, and $\langle \mathbf{B} \rangle$ is given by the Archimedian spiral Parker field. The plasma is assumed to be mirror symmetric. A further approximation, less well justified (Carbone et al 1994, Matthaeus et al 1990), but needed to make the problem tractable, is to assume a form for the three-dimensional spectral tensor. The common forms used are slab, isotropic, two-dimensional, or axisymmetric.

As an illustration, for the isotropic case, the equations describing the evolution of inward and outward-propagating fluctuations can be written as (Oughton 1993):

$$\left[\frac{\partial P^\pm}{\partial t} + (U \mp V_{Ar}) \frac{\partial P^\pm}{\partial R} \right] + \left(\frac{U \pm V_{Ar}}{R} \right) P^\pm + M^\pm F = NL^\pm$$

$$\left(\frac{\partial F}{\partial t} + U \frac{\partial F}{\partial R} + \frac{U}{R} F \right) + 2(P^- M^+ + P^+ M^-) = NL^F. \quad (16)$$

The first terms on the left-hand-side describe the linear evolution of P^\pm (the power in z^\pm) and F (essentially the difference between the kinetic and magnetic energy spectra), the second term in the first of the equations is the WKB approximation, and the last term on the left-hand side contains the terms describing mixing of the inward and outward-propagating fluctuations. The right-hand side of Equation (16) contains the small-scale nonlinear terms that include the

diffusive flow of energy in Fourier space. The mixing terms, M^\pm , are given by

$$M^\pm = \frac{\alpha}{\alpha + 2} \frac{1}{2R} \left[U \mp \left(\frac{4}{\alpha} - 1 \right) V_{Ar} \right], \quad (17)$$

where α is the index of the power spectrum of the total energy and V_{Ar} is the radial component of the Alfvén velocity.

The nonlinear terms on the right-hand side of Equation (17) must be modeled before the equations can be solved. The terms NL^\pm and NL^F describe complex turbulent phenomena that are not well understood in inhomogeneous media. Assuming that the separation of scales is valid, it is possible to treat the turbulence locally using homogeneous theory and phenomenological models (Marsch & Tu 1993; Verma 1994; Zhou & Matthaeus 1990a,c). Because the inertial range is treated incompressibly, one can follow, for example, Kolmogoroff's approach for NL^\pm as outlined above. Modeling NL^F is more difficult because less is known about it (e.g. F is not even a conserved quantity). Oughton (1993) treats this term phenomenologically by dividing its time variation into two terms, one describing the tendency for r_A to become less than one, and the other tending to enforce equipartition and driving F toward zero. The model is completed by energy input from the low- k end of the inertial range using Kolmogoroff's hypothesis for the decay of the energy-containing eddies (Batchelor 1970, Matthaeus et al 1994). The resulting set of equations then forms a closed system that can be integrated numerically to give the evolution of the power spectra with heliocentric distance.

3.6 *Nearly Incompressible Turbulence*

Application of the standard Kolmogoroff arguments to weakly compressible hydrodynamics predicts an omnidirectional pressure spectrum with power-law index $\alpha = -7/3$ (Batchelor 1951, George et al 1984). A linear (perturbative) relationship between pressure and density would imply a $-7/3$ spectral index also for the density, which is at odds with the observed spectral index of $\alpha \approx -5/3$. A treatment of density spectra for MHD was proposed by Montgomery et al (1987), who showed that under certain circumstances the expected spectral index was $-5/3$ if the magnetic (component) fluctuation spectrum index had this value. This tracking of the magnetic spectrum by the density spectrum emerges at high wave numbers and is essentially a statistical form of pressure balance between thermal and magnetic pressures (Shebalin & Montgomery 1988). The theory requires low turbulent Mach number M and bounds on acoustic activity in the initial data, but does not require the special geometry of velocity fluctuations that are needed for exact (static) pressure balance. Further elaboration of these ideas has led to a theory of "nearly incompressible MHD" (Matthaeus & Brown 1988; Zank & Matthaeus 1990, 1992a), which describes the nature of compressible MHD solutions in the limit of low turbulent acoustic Mach number ($M_s = \delta v/c_s$). Conditions for these flows to approach solutions

to the incompressible equations are obtained by carrying out a systematic two-time-scale, two-length-scale expansion of the compressible equations using the turbulent Mach number as a small parameter. This theory has important antecedents in the hydrodynamic theory of acoustic wave generation by vortical flows (Lighthill 1952) and in the rigorous connections that have been established between low Mach number and incompressible hydrodynamics (Klainerman & Majda 1982).

For conditions in which near-incompressibility is obtained, the lowest order solution is identical to the corresponding solution of the incompressible MHD equations, with higher order terms providing the compressive modifications. At low M_s the slow time scale is associated with the incompressive fields and the fast scale is associated with acoustic modes. When acoustic modes have sufficiently small amplitude in the initial data, the density fluctuations are non-propagating and are enslaved to the incompressive fields. Although simulations have shed some light on the extent of applicability of nearly incompressible theory for hydrodynamics (Ghosh & Matthaeus 1992), the analogous study for MHD has yet to be conducted. Discussion of solar wind observations in terms of the earlier (high β —the ratio of thermal to magnetic pressures), nearly incompressible theory can be found in Matthaeus et al (1991), who focused on the “pseudosound” character of density fluctuations presented by Montgomery et al (1987). Tests of the expected scaling of the density fluctuation amplitude with Mach number ($\delta n/n \propto M_s^2$) for a polytropic equation of state have had limited success, although at very low M_s in the outer heliosphere the scaling appears to work well (Matthaeus et al 1991). In the inner heliosphere, even at solar minimum, the situation is more complex (Grappin et al 1991, Klein et al 1993a) with $\delta n/n \propto M_s$ between the high-speed streams and both M_s and M_s^2 scaling in the high-speed wind regions. This is to be expected since the turbulence is in general less developed and the density “fluctuations” in the striated regions probably result mainly from initial conditions rather than dynamical evolution. Nearly incompressible theory also allows for $\delta n/n \propto M_s$ in flows for which the density and temperature are anticorrelated (Zank et al 1990), but it is unclear how frequently this occurs in the solar wind. The nearly incompressible formulation of MHD has somewhat distinctive properties in the cases of high and low plasma β (Zank & Matthaeus 1993). For example, one interesting implication is that nonpropagating density fluctuations are expected to be anisotropic (quasi-two dimensional) for $\beta \approx 1$ with the propagating density fluctuations isotropically distributed. In contrast, for $\beta \ll 1$ the propagating acoustic waves also become anisotropic. The latter case would be more appropriate in the lower corona where Coles et al (1991) have reported some indication of elongated density fluctuations. A number of other implications of this theory for solar wind observations have been discussed by Zank & Matthaeus (1992b).

4. CENTRAL ISSUES AND PROBLEMS

4.1 *Origin Near the Sun: Photospheric Motions, Reconnection, or Shear?*

Although many aspects of the properties and evolution of solar wind turbulence are fairly well understood, nonetheless fundamental problems remain, often associated with unexplored regions in the heliosphere. In particular, we do not know where in the solar atmosphere the initial population of solar wind fluctuations originates, nor do we know the source of free energy, nor how the fluctuations evolve up to the Alfvénic critical point. Velli et al (1991), Velli (1993), and Krogulec et al (1994) have reported work on the wave propagation problem in the lower corona, and Mullan (1990) has reviewed the observational evidence pertaining to sources of small-scale structure.

The propagation theories predict a frequency-dependent reflection coefficient with possible resonances and even trapping of the waves that one might expect to produce observable spectral features, which are not seen (Tu et al 1990). In large, relatively uniform regions removed from sector boundaries and stream interfaces, the observed spectrum from the scale of days to minutes is a featureless power law with spectral index $\alpha \approx -1$. The scale of a day is that of the transit time to the spacecraft, and thus this regime is linked to boundary conditions. Various ideas have been advanced for producing an f^{-1} spectrum in an expanding, turbulent medium (e.g. Velli et al 1989), but these mechanisms all meet the same objection that the plasma will have much less than one eddy-turnover time to evolve and the structures involved are too big to fit in the “box” between the Sun and the point of observation (Zhou et al 1990). Moreover, cascade mechanisms generally produce steeper spectra ($\alpha \sim -5/3$).

There are, however, observed structures in the photosphere and lower corona that almost certainly influence the generation of the initial population of fluctuations. These include filaments, polar plumes, and X-ray bright points. The simple model in which motions in the photosphere wiggle the ends of the field lines like rubber bands is probably ruled out by the f^{-1} spectrum in that the motions required to produce such a spectrum appear chaotic, whereas the observed motions in the photosphere are quite smooth. It is difficult to imagine how the spectrum could become flatter as the fluctuations propagate through the corona. Moreover, such an evolution would decrease the already low power available from the footpoint motion. The lower corona is the more probable region for the origin of the fluctuations, as, for example, magnetic reconnection there can produce turbulent fluctuations directly (Matthaeus & Lamkin 1986). Matthaeus & Goldstein (1986) argued that a superposition of power-law distributed fluctuations from uncorrelated sources would lead to an f^{-1} spectrum in the solar wind provided that the correlation scales of the differing sources are log-normally distributed. The particular model they presented is based upon

a scale-invariant distribution of structures produced by magnetic reconnection in the lower corona. There is no direct evidence for such a reconnection cascade; however, the basic idea of scale-invariant superposition might be applied to other dynamical processes as well. Feldman et al (1993) suggested that the observation of ion jets in the solar wind is consistent with a reconnection source (described by others as “microflares” and “nanoflares”; see Parker 1990) near the transition region in the solar atmosphere. This nanoflare energy flux could possibly contribute to both the acceleration of the high-speed streams and to the production of fluctuations. Even without reconnection, the corona may be as filamentary in its velocity structure (“microstreams”) as it is observed to be in its density structure. The shears between stream tubes could then lead to fluctuations and a concomitant reduction in the shear gradients. Clearly, very structured flows in the inner heliosphere are associated with highly developed turbulence spectra (Klein et al 1993b).

4.2 *The Role of Expansion in the Evolution of Fluctuations*

From the standpoint of the heliosphere as a whole, the Sun is nearly a point source of plasma, and thus the flow expands roughly spherically. This expansion dominates all other effects in determining the mean field magnitude and direction, the amplitude of the fluctuations, and the temperature of the plasma. The effect of expansion on the fluctuations should be quite different depending on the relative size of the disturbance and the scale for gradients in plasma properties. Gradients will have little effect on disturbances whose scale lengths parallel to the large-scale gradients are small. The gradient scale varies as the distance from the Sun [e.g. $(1/U)\nabla \cdot \mathbf{U} = 2/R$, where \mathbf{U} is a constant radial expansion speed], and thus the expansion will affect a wider range of scales closer to the Sun. Two limiting cases are of particular interest: parallel-propagating Alfvén waves (i.e. “slab” geometry) and structures or turbulence with wave vectors perpendicular to the Parker field (i.e. “two-dimensional” geometry). Exactly perpendicular wave vectors are nonpropagating, convecting structures that are a combination of quasi-two dimensional turbulence and field-aligned filamentary structures originating near the solar surface; these appear in coronal photographs as polar plumes or as strong density contrasts in helmet streamers (Koutchmy 1988).

The recent work by Marsch & Tu (1993), Zhou & Matthaeus (1990a,b,c), and Oughton (1993), which combines evolution of waves in the large-scale flow with modeling of turbulence in the inertial range, is now being tested against observations. The driving term in Equation (15) or the mixing term in (16) becomes large when the phase interference between the outward and inward-propagating waves becomes small enough for reflection or mixing to become important (Zhou & Matthaeus 1990b). This happens if the fluctuations are strongly turbulent and thus no dispersion relation exists. The driving terms can also be large when k becomes small, when V_A becomes small (as it must over

the poles of the Sun; see Jokipii & Kóta 1989), or when \mathbf{k} becomes nearly perpendicular to $\langle \mathbf{B} \rangle$ (convected filamentary structures). As pointed out by Jokipii & Kóta for the low field case, the main effect of a small value of $\mathbf{k} \cdot \mathbf{V}_A$ is that the tension in the background magnetic field lines can be ignored. In this case, neglecting compression, velocity and magnetic fluctuations transverse to the magnetic field evolve independently according to their own conservation laws. As shown by Tu & Marsch (1993), the conservation of transverse magnetic flux and vorticity implies that both the velocity and magnetic fluctuations have $1/r$ dependences on heliocentric distance, and thus, when measured in Alfvén speed units, magnetic field fluctuations are constant with distance, the Alfvén ratio is proportional to r^{-2} , and

$$\sigma_c \propto \frac{r^{-a}}{r^{-2a} + \text{constant}}, \quad (18)$$

with $a = 1$.

Behavior of this type for the radial evolution of the cross helicity, the Alfvén ratio, and the kinetic and magnetic energies can be obtained from scale-separated spectral transport theory (Zhou & Matthaeus 1990c, Oughton 1993, Tu & Marsch 1993) under a variety of approximations. Simple analytic solutions emerge only when nonlinear coupling effects are ignored or treated implicitly. For a number of different cases the normalized cross helicity behaves as in Equation (18) with a generally in the range of about $1/6$ to 1 . Zhou & Matthaeus (1990c) showed that $a = 1$ for a slab model (cf Heinemann & Olbert 1980) in the weak magnetic field ($V_A \rightarrow 0$) limit. For isotropic fluctuations, also neglecting large-scale magnetic field effects, Zhou & Matthaeus (1990c) found $a = 5/11$ for a Kolmogoroff $-5/3$ spectral index. The $k = 0$ slab model is identical to the two-dimensional fluctuation model, even when large-scale propagation effects are not ignored (Tu & Marsch 1993). Numerical solutions for two-dimensional fluctuations including large-scale propagation effects show a radial decrease of σ_c only slightly slower than the above case with $a = 1$ (Oughton 1993). Thus, for large-scale parallel-propagating Alfvén waves or two-dimensional fluctuations with wave vectors nearly perpendicular to the magnetic field, the magnetic energy should quickly become dominant and the cross helicity should disappear with increasing radial distance. The isotropic assumption gives a qualitatively similar effect when the large-scale magnetic field is ignored, but when it is included the reduction of cross helicity is greatly suppressed (Oughton 1993). In effect, isotropic fluctuations act very much like shorter wavelength slab fluctuations, which are accurately described by WKB theory.

The appearance of very different radial evolution for small-scale disturbances with wave vectors parallel to the magnetic field and fluctuations at any scale perpendicular to the magnetic field suggests that much of the seemingly turbulent evolution of the solar wind fluctuations arises from expansion alone

(Oughton & Matthaeus 1992, Tu & Marsch 1993, Zhou & Matthaeus 1990c). If we suppose that both components were superposed near the Alfvénic critical point, then the right mix could lead to cross helicity evolution similar to that observed, as well as to correlation functions peaked parallel and perpendicular to the average magnetic field (Matthaeus et al 1990). The magnetic fluctuations of the convected filamentary structures decay more slowly than do those of parallel waves, and thus the structures should become more dominant with increasing distance from the Sun and the Alfvénicity will decrease with distance. Supposing that the structures have a well-developed turbulence spectrum, it might be possible to make this model fit the observed spectral evolution as well; the increasing dominance of the structures would lead to increasingly Kolmogoroff-like spectra.

However, the linear superposition model neglects important effects. The value of r_A , rather than approaching zero as expected for pure two-dimensional fluctuations, never goes below 0.5, on average (Roberts et al 1990). Transport models can be extended to include this tendency toward equipartition, as shown by Oughton (1993) who found that even for pure two-dimensional fluctuations, the mixing effect is nullified to a large extent. For specific forms of the model, σ_c decreases only to a level of about 0.8 by 2 AU. Thus, it appears doubtful that the observed reduction of σ_c can be accounted for fully by an approach in which the mixing of inward and outward sense of cross helicity is produced solely by expansion.

Both Tu & Marsch (1993) and Oughton (1993) also point out that a superposition model predicts that the observations should show a dependence on the angle between the solar wind velocity and the mean magnetic field. For example, near 1 AU, r_A should be small when the field is nearly tangential and near 1 when it is radial because the spacecraft only samples wave vectors along the wind direction. However, it is clear from *Helios 2* primary mission data obtained between 0.75 and 1 AU that no correlation exists between r_A and direction of \mathbf{B} . The cross helicity in this model should be uniformly low in the outer heliosphere, but there are regions, such as the example observed near 8 AU seen in Figure 3 toward the end of the interval (see also Roberts et al 1987b, figure 7b) that are highly Alfvénic with $r_A \approx 1$, although the field is in the tangential direction.

These considerations imply that although there should be a tendency for \mathbf{k}_\perp structures to produce reductions in cross helicity, other processes dominate the linear effects. This also seems to be the case for large-scale parallel Alfvénic fluctuations in that $r_A \approx 1$ for the transverse fluctuations at large scales in radial mean magnetic fields in the inner heliosphere. It is true that the cross helicity of the such fluctuations decays rapidly, more or less according to what might be expected from Equation (18); perhaps this is due to phase shifts coming from the gradients rather than the decay of the velocity field. The fluctuation amplitude

evolution was recently studied from a very general viewpoint by Verma & Roberts (1993), who found that any fluctuations about time-averaged fields would evolve at nearly the WKB rate if r_A were held fixed in a range about the observed values and the band of fluctuations in k -space had no net dissipation. This is consistent with the observed evolution of the amplitudes in the inner heliosphere at large scales (Roberts 1989) and again implies that the large scales (as long as a day or so in the spacecraft frame) do undergo some nonlinear interactions that maintain near equipartition of the magnetic and velocity fields. Although further study is needed to determine the full range of effects possible in a scale-separated transport model, it seems fairly certain at this point that the expansion effects contained in the linear transport models cannot explain completely the observed radial evolution of solar wind fluctuations.

4.3 *Shear: General Cascade Driver or Localized Mixer?*

While it is clear that velocity shear plays an important role in the evolution of solar wind fluctuations, it is not clear, however, whether velocity gradients produce local effects only or if they globally control the cross helicity, Alfvén ratio, and other physical parameters (Bavassano & Bruno 1989a, Klein et al 1993b). Simulations can help to determine the relative importance of shear compared with compression and expansion, but no systematic comparisons have been made of the relative importance of the global expansion and local velocity gradients in controlling the cross helicity and Alfvén ratio evolution. In this section we concentrate on the role of shear alone as studied using incompressible MHD simulations of a nonexpanding flow.

The numerical simulations we discuss progress from a simple two-dimensional velocity shear layer to a three-dimensional situation that includes both velocity and magnetic shear (Roberts et al 1991, 1992). In the simplest case, no energy was input above the low wave number coherent modes used to define a weakly varying magnetic field and two velocity shear layers, while random noise (1% of the energy) initiated the nonlinear evolution. The energy in the mean field nearly equaled the fluctuating energy, and the value of σ_c was initially only 0.12. Although the strong mean field and the relatively large width of the shear layer made only the longest wavelength Kelvin–Helmholtz unstable, the wave number spectra of both magnetic energy and kinetic energy evolved rapidly. Within a single eddy-turnover time, a significant amount of energy was cascaded to high- k modes. The physical time scale of this evolution was estimated roughly by dividing the correlation length of fluctuations at 1 AU of about 5×10^6 km (Matthaeus & Goldstein 1982a) by a typical rms speed fluctuation of ≈ 100 km/s for scales that include streams to find a characteristic time of about a day. Thus, the wind can convect to 1 AU within a few eddy-turnover times, and the simulations suggest that this is enough to form a well-developed power law spectrum. The initially small global σ_c in the simulations remained small and the inertial range σ_c fluctuated about zero, indicating that the cascade

of energy from large scales favored neither “outward” nor “inward” propagation (Bavassano et al 1978). In addition, the Alfvén ratio r_A was close to one. Thus, although the velocity shear instability can generate a nearly equipartitioned spectrum of fluctuations, it cannot produce the outward traveling Alfvén waves characteristic of the inner heliosphere, in contrast to the idea presented by Matthaeus et al (1984).

To study the effect of velocity shear on initially highly Alfvénic fluctuations, we added an isotropic high wave number power-law distribution of Alfvénic modes with maximal cross helicity to the shear modes. In this case, σ_c systematically decreased at high wave numbers, as noted observationally by Roberts et al (1987a), and the Alfvén ratio r_A remained close to unity throughout the run. Hence, velocity shear appears capable of decreasing the cross helicity of the small-scale fluctuations. As the magnitude of the background magnetic field increases, these effects become weaker; the cross helicity evolution essentially stops for sufficiently large $\langle \mathbf{B} \rangle$ as the interactions become increasingly linear (Grappin et al 1982, Matthaeus & Zhou 1989). For strong background magnetic fields, r_A approaches 1, larger than the typical solar wind values of 0.5.

Although the cross helicity evolution in the simulations is associated closely with the strong shear layers, the decrease in the solar wind is nearly ubiquitous. Small amounts of shear certainly exist within streams, however, and to address the role of small disorganized velocity shears, Roberts et al (1992) designed simulations that did not contain any organized shear layers. In a decaying example, the large-scale cross helicity was zero, while in a driven run the effect of the larger scales on the initially Alfvénic population was modeled as a forcing in a low- k band of wave vectors by adding uncorrelated $\delta \mathbf{v}$ and $\delta \mathbf{B}$ increments to low- k modes. In both sets of simulations, the observed changes in σ_c resembled those seen in the earlier cases containing large-scale shear; namely, the initially large high- k cross helicity gradually decreased as the run proceeded, indicating that even small, but nontrivial, velocity shear affects initially highly Alfvénic flows.

In Roberts et al (1991), these studies were further generalized by including a fairly narrow “low-speed stream” surrounded on either side by high-speed streams with a current sheet embedded in the middle of the slow wind, thereby mimicking solar wind conditions at solar minimum. The initial population of purely Alfvénic fluctuations at high k was given a flat spectrum (modal spectral index -1). Figure 7 shows one-dimensional energy spectra in terms of Elsässer variables for the solution. In the top panel the dominant “outward-propagating” (z^+) fluctuations relax rapidly toward a steep spectrum, and then evolve slowly, similar to the observed spectra (Marsch & Tu 1990a) shown in Figure 6 (see also the evolution of δz^+ and δz^- in Figure 2b). Shear-driven turbulence produces nearly equal large-scale input of both z^+ and z^- . The z^- energy attains a steady state matched by dissipation, whereas z^+ dissipates due to the flat input

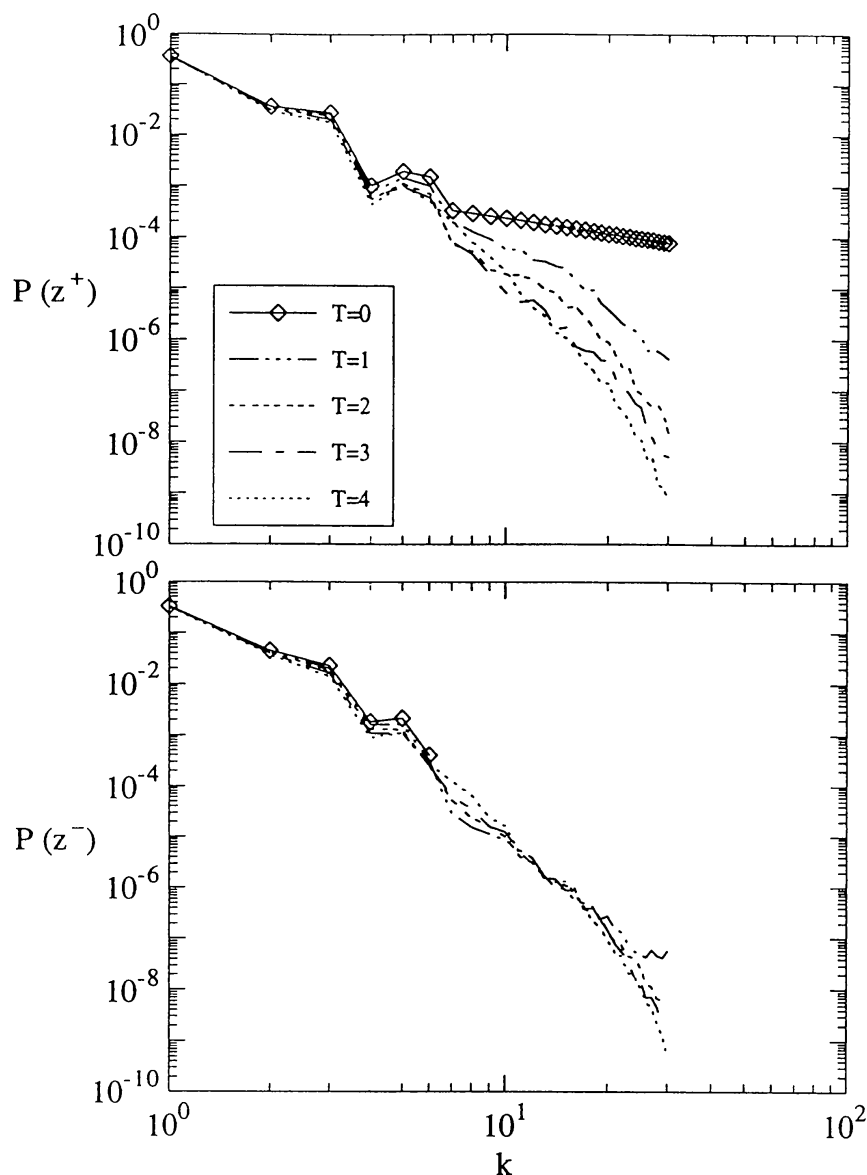


Figure 7 Time evolution of the power spectra of the Elsässer variables z^+ and z^- for the incompressible MHD simulation that modeled the heliospheric current sheet. (From Roberts et al 1991.)

spectrum of z^+ power at high k . In the outer heliosphere the z^+ and z^- spectra are observed to evolve gradually toward each other, presumably with a slow cascade matched by slow dissipation (Roberts et al 1987a,b), and this quasi-steady state leads to an evolution of the amplitudes that closely resembles that of dissipationless Alfvénic turbulence (Roberts et al 1990, Verma & Roberts 1993). In Figure 8 we show Elsässer spectra constructed from the simulation for a typical cut in x in the middle of the “high-speed stream,” and for a cut near the current sheet—the “low-speed stream.” We see the characteristic “breathing”

(cf Figure 5) seen in the observations as described by Grappin et al (1990) and Marsch & Tu (1990a), although the z^- increases somewhat more here than is observed. Spectra for a cut near the current sheet at the edge of the box, in the middle of the high-speed stream look very much like the low-speed stream spectra, indicating that proximity to the current sheet is the critical factor and not the speed of the wind or even the proximity to shear layers.

The spatial structure of the fluctuations can be analyzed by filtering out the low wave number power. At $T = 1$ for the “solar minimum” case, σ_c calculated by local correlations of these “high-pass” fields deviates significantly from $+1$ at the location of the current sheets rather than where the vorticity is large. By contrast, without current sheets the strong shear layers are the dominant source of the evolution. Figure 9 shows the spatial evolution of B_x , V_x , σ_c , and ω for the incompressible simulation with current sheets, as described in Roberts et al (1991). The top panel of the figure shows that the field and vorticity structure have been maintained on average, but that σ_c at high k (originally $+1$ everywhere) has significantly decreased in the region of the current sheets near the edge and the middle of the box and especially so when the current sheet is near the strong velocity shear layers. This effect is observed in the solar wind (Figure 2*b*, second panel from the top). By $T = 4$, the cross helicity is low everywhere, on average, although both positive and negative regions contribute. There is no significant spreading of the current sheet region, considered as bounded by the vorticity layers, as would be required in a “spreading turbulent wake” picture (Grappin et al 1991).

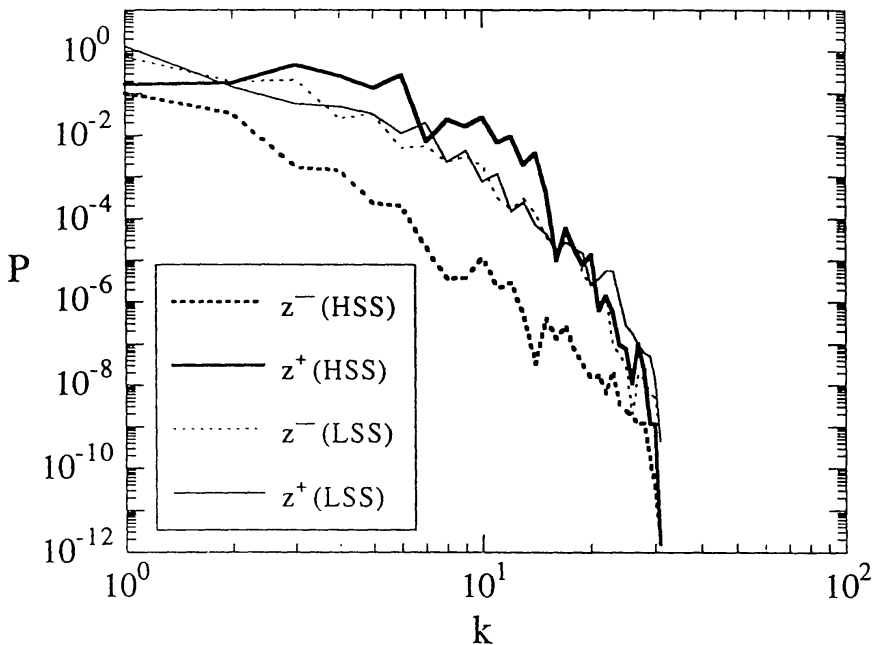


Figure 8 Elsässer spectra for high- and low-speed streams taken from cuts along x in the simulation box. (From Roberts et al 1991.)

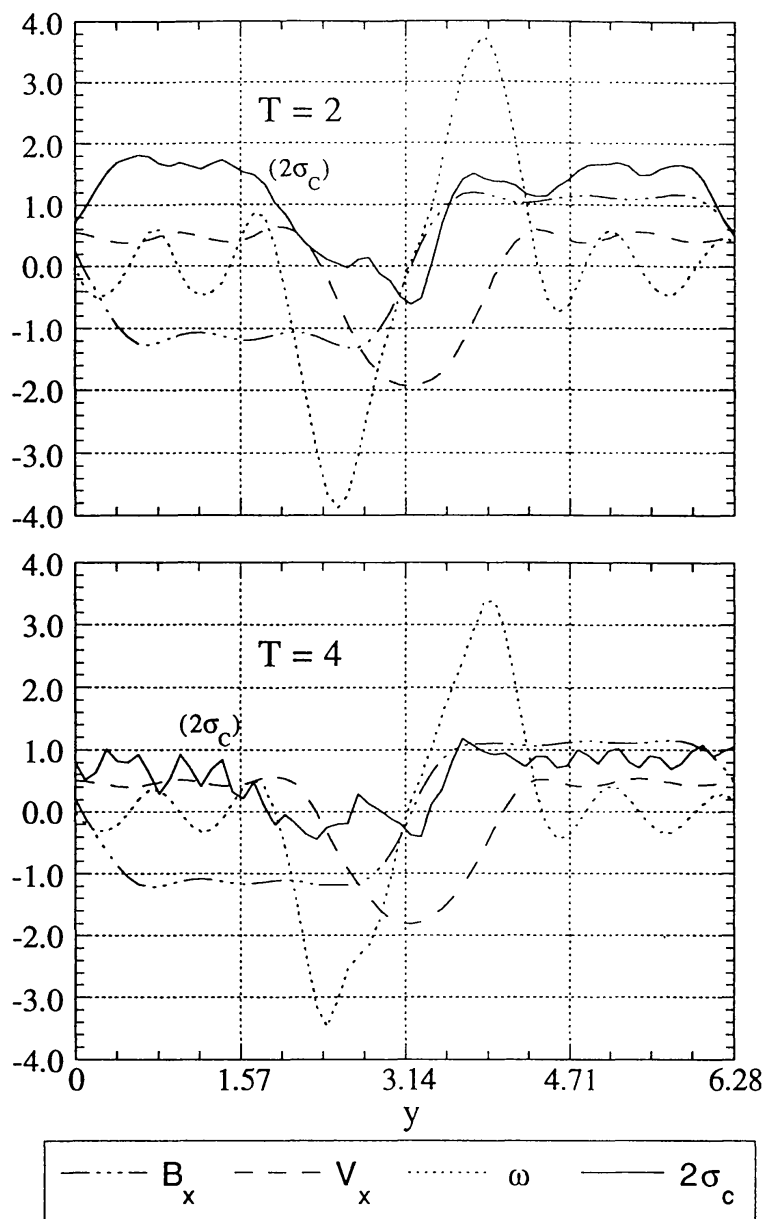


Figure 9 Quantities averaged over x at $T = 2$ and $T = 4$ for the incompressible run with current sheets. (From Roberts et al 1991.)

Two-dimensional simulations model the heliospheric current sheet by setting the magnitude of the magnetic field equal to zero at the center of the sheet. However, observations show that the field magnitude rarely decreases by more than 20%, but instead rotates out of the meridional plane as it changes direction. To determine whether the decrease in cross helicity in the two-dimensional simulations is caused by the near-zero value of magnetic field or results because of the diminished ability of a transverse (to the flow) magnetic field to stabilize velocity shear instabilities, Stribling et al (1994c) performed a series of three-

dimensional (incompressible) simulations of the solar heliospheric current sheet at solar minimum. The runs had resolutions as large as 128^3 with Reynolds numbers of 1000, and were carried to 5 eddy-turnover times. The evolution of the cross helicity was essentially identical to that seen in two dimensions. As before, σ_c was depleted within the regions of velocity and magnetic shear, while outside the shear layers the flow remained highly Alfvénic for a longer time. Consequently, it appears that the change in direction of the magnetic field in the center of the current sheet, not its magnitude, is controlling the cross helicity evolution. A similar evolution of cross helicity near the current sheet occurs when transverse expansion of the flow is included (Grappin et al 1993a).

4.4 *Compressive Structures: Scattering Centers or Along for the Ride?*

Compressions of the solar wind plasma arising from velocity differences are common features, but their importance to the overall evolution of solar wind fluctuations has yet to be determined. The effects of compressive flows on large-scale fields are obvious with increasing heliocentric distance: Fast streams overtake slow streams, producing compressed “interaction regions” containing increased density, temperature, and magnetic field strength. Beyond 1–2 AU these regions form forward and reverse shocks, but the compression is usually isentropic until then. Belcher & Davis (1971) considered interaction regions to be where waves were amplified or generated, and indeed wave amplitudes are higher there. They also argued that the Alfvénicity should be lower in these regions due to the generation of both inward-propagating Alfvén waves and compressive fluctuations. Although they observed the expected correlation, more extensive analyses by Roberts et al (1987a, 1990) showed that there is usually only a small additional depletion of cross helicity in interaction regions in the outer heliosphere, and that the increased amplitudes of the fluctuations, which arise long before shocks form, were correlated most strongly with the compression of the average magnetic field. Thus, local generation does not appear to be significant.

Compressive effects, however, may be significant in other ways. In particular, the level of the small-scale z^- fluctuations is correlated with relative density enhancements, and especially at solar minimum, the regions with highly structured density and other plasma properties show both highly developed turbulence spectra and strong cross helicity depletion (Bavassano & Bruno 1989; Grappin et al 1991; Marsch & Tu 1989; 1990a,b). Moreover, the spectra of density, temperature, magnetic field strength, and z^- all show similar flattening at the high wave number end of the inertial range, implying links between them. An enhancement at high wave numbers of the minority z^- was predicted by Grappin et al (1983) for incompressible turbulence, and thus it is possible that this is the primary effect that drives the others. Perhaps most puzzling is

the observation that z^+ fluctuations are somewhat better correlated with temperature than with any other indicator of macroscale structure (Grappin et al 1990).

These observations have led to various ideas for the importance of compressive effects, including the suggestion that the structures perpendicular to the field represent non-Alfvénic disturbances that are convected with the wind and that the Alfvénic fluctuations interact dynamically with these to produce the observed cross helicity evolution (Klein et al 1993a,b). It is also possible that the regions observed to be structured in “compressive” quantities were also highly striated in velocity as well near the Sun. Evidence for this is provided by radio occultation measurements that at least hint at regions of very strong fast and slow flow differences within what is nominally a single stream (Lotova 1988).

An alternative viewpoint maintains that the smaller-scale compressive effects are results rather than causes. Early observations showed that compressive structures are frequently nearly pressure balanced (Burlaga & Ogilvie 1970). Later observations have shown this is to be true to very fine scales (Roberts et al 1987a). Moreover, the tendency for pressure balance becomes greater with increasing heliocentric distance (Roberts 1990, Vellante & Lazarus 1987). Both interstellar and interplanetary density spectra tend to have $-5/3$ spectral indices, and the observed values of the relative density fluctuations are usually small (about 0.1) outside of the highly structured regions near the Sun. An explanation of the density spectra in terms of the quasi-pressure-balance viewpoint was given by Montgomery et al (1987).

The nearly incompressible viewpoint is supported to some extent by simulations. For example, a compressible MHD simulation (Roberts et al 1991) with current sheet, an initial turbulent sonic Mach number of 0.3, and $\gamma = 5/3$, yields nearly identical evolution of the “incompressible” quantities σ_c , v_x , and b_x as was found in the incompressible case (see Figure 10). The new features were a persistent anticorrelation between the magnetic field magnitude and the density ($\rho_{B,n}$), suggestive of nearly pressure-balanced “pseudo-sound” (Matthaeus et al 1991) and a density fluctuation that correlated well with the fluctuations in z^- . This correlation had been pointed out previously (Bavassano & Bruno 1989, Bruno & Bavassano 1991, Grappin et al 1990), and it had been argued that the higher compressions indicated an essential role for compression in understanding the plasma evolution. The present simulations indicate that, on the contrary, these density fluctuations arise naturally from the incompressible evolution (Matthaeus et al 1991, Montgomery et al 1987).

The simulations also show essentially the correct behavior of r_A . The values of r_A , found by calculating ratios of fluctuating energy in small boxes in the simulation domain, remain near 1, and although the mean value is very close to 1 at $T = 2$ (higher than the observed 0.5), the distribution of r_A values

is strongly peaked near 0.5. There are regions of lower r_A associated with low cross helicity regions such as were recently reported by Tu & Marsch (1991). Although there is no simple association between r_A and σ_c in either the simulations or observations, both quantities tend to have low values in regions that are more strongly developed, and both tend to be near +1 in more purely Alfvénic regions, as expected.

A major failing of the above simulation is that the anticorrelation of density and magnetic field strength is most pronounced in the region near the current sheet—just the opposite of what is observed here. It is likely that the structures responsible for this anticorrelation are convected from the Sun and thus should be in the initial conditions. The observations indicate that the initial predominance of the pressure-balanced structures near the current sheet is eroded, but that farther out the $\rho_{B,n}$ anticorrelation returns as the plasma relaxes into a state consistent with dynamically enforced pressure balance. Further simulation efforts will be needed to decide if this scenario is correct.

A second important problem with the simulations is that the shear regions are much too broad compared to observations. As remarked by Bavassano & Bruno (1989), this leads to difficulties because waves cannot propagate away from the observed narrow stream interfaces fast enough to produce cross helicity depletions at the required distances from the interfaces. For the shear picture to

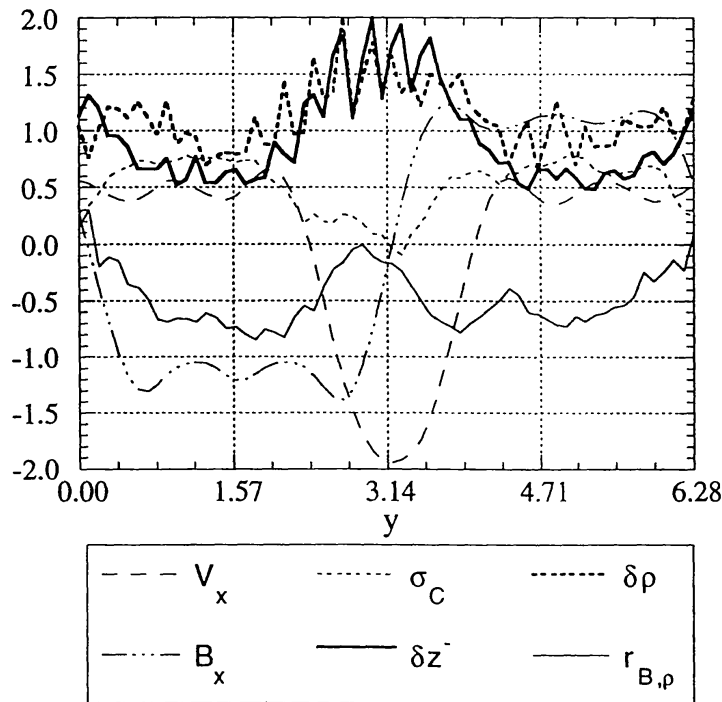


Figure 10 Quantities averaged over x at $T = 2$ for the compressible run with current sheets. The density and z^- fluctuations are normalized to twice their maximum values (0.042 and 0.075, respectively). (From Roberts et al 1991.)

be valid, either small shears must affect the plasma or larger shears must have existed closer to the Sun. The former possibility holds at least to some extent: The simulations show that shear well below the threshold for Kelvin–Helmholtz instability produces significant nonlinear effects. It may be, however, that for the turbulence to become as well developed as observed in the plasma sheet region, microstreams must pervade the striated regions in the corona. On the other hand, the explanation for the well-developed spectra may lie in the initial conditions; in the interaction of the Alfvénic population with the convected, striated structures; or in compressive effects.

4.5 *Dissipation and Heating: The Problem of Solar Wind Acceleration*

Coleman (1968) first suggested that the solar wind was heated by turbulent evolution. His idea has been revisited by Tu et al (1984) and Tu (1988) who embedded either Kolmogoroff or Kraichnan-type nonlinear inertial range phenomenology into the spatial transport framework of WKB theory. Tu (1987) also utilized the same basic approach in a calculation of solar wind heating, including feedback on the large-scale fields. Another approach to modeling the effects of turbulent dissipation and heating on the acceleration of the wind was made by Hollweg (1986) and Hollweg & Johnson (1988), who employed nonlinear phenomenology appropriate to the energy-containing range of hydrodynamic turbulence, along with a WKB transport equation. Both of these approaches showed, at least roughly, that turbulent heating was consistent with the observed spectral evolution in the inner heliosphere, taking into account the dissipation of the fluctuations by a cascade and the general decay of the fluctuations due to expansion. However, these solar wind models fall short of providing a quantitative explanation of heating and acceleration, as pointed out, for example, by Isenberg (1990) and Matthaeus et al (1994). The models by Tu and Hollweg might be improved by extension of the spatial transport formalism from WKB theory to a full multiple-scales treatment. Another aspect of heating models that requires further development is the phenomenological treatment of the nonlinear effects. Currently, there are several efforts to evaluate and improve upon the simple nonlinear models that have been used by Tu et al (1984), Tu (1987, 1988), Zhou & Matthaeus (1990b), and Matthaeus et al (1994). The development of these models falls into two general classes: models for the energy-containing range of fluctuations (Hollweg 1986, Hollweg & Johnson 1988, Matthaeus et al 1994) and models for the inertial range of the fluctuations (Tu et al 1984; Tu 1987, 1988; Zhou & Matthaeus 1990b).

More recently, Verma (1994) and Verma et al (1995) used the phenomenologies discussed in Section 3.3 to evaluate the role of turbulent dissipation in the inner and outer heliosphere. They found that there was no simple, consistent set of cascade constants that would fit all the data for both Alfvénic and non-

Alfvénic streams, but in many cases the predicted heating had to be suppressed to account for the observed evolution. Power laws for temperature versus distance comparable to those observed were not difficult to generate. The lack of a completely self-consistent model is troublesome, but Verma also found that the predicted cascade rates do not agree in detail with simulations, especially at high cross helicity, and thus there is reason to believe that the nonlinear terms have yet to be properly modeled.

Other studies (Matthaeus et al 1993, Pontius et al 1993) have focused on various models of nonlinearities that affect the larger scale energy-containing eddies in the solar wind, which likely provide the energy source that drives the inertial range cascade. By comparison with decaying three-dimensional MHD simulations, Pontius et al (1993) concluded that phenomenological models work reasonably well in predicting the overall decay of Elsässer energies and the energy difference (kinetic minus magnetic). However, the greatest difficulties in the energy-containing models occur when the cross helicity is fractionally large compared with the fluctuation energy. This is consistent with a similar deficiency found by Verma (1994) for inertial range cascade models. Unfortunately, the high cross helicity parameter regime is precisely that which is most relevant to solar wind evolution in the inner heliosphere and to the problem of acceleration. Therefore, further development is needed in these areas. Given the uncertainties involved, turbulent heating remains a likely source of significant heating well into the outer heliosphere. From the work of Burlaga et al (1994), we know that during 1986–1989 few shocks were observed between 18.9 and 30.2 AU; thus shocks cannot be responsible for heating solar wind protons at these distances and times. [Whang et al (1991) showed that shock heating is consistent with observations between 1 and 15 AU.] One possibly viable alternative to turbulent dissipation is the interaction of the solar wind with interstellar neutrals.

Because standard thermal models of the solar wind fail to explain the observed mass flux, density, and temperature at 1 AU, dissipation of Alfvén waves generated near the Sun has been invoked as the means by which high-speed solar wind streams are accelerated. A fundamental problem with these models is that the wave amplitudes observed between 0.3 and 1 AU, if adiabatically extrapolated back to the Sun, would be insufficient to accelerate the wind despite their being a substantial fraction of the background Parker field (Hollweg 1975, 1978; Roberts 1989). Many models have invoked “saturation” to circumvent this difficulty. In this view, the relative amplitude of the transverse wave fluctuations increases with increasing heliocentric distance, as predicted by the WKB approximation, until $\delta B/B$ is order unity when “nonlinear effects” lead to dissipation and maintain $\delta B/B$ of order unity. One possible mechanism for accomplishing this dissipation is for large amplitude waves to generate density fluctuations via a parametric process or more directly through intrinsic $|B|$

fluctuations. Those density fluctuations can then dissipate via Landau damping. Alternative models (Hollweg & Johnson 1988, Isenberg 1990) invoke turbulence to dissipate the waves, although with limited success in achieving a self-consistent picture of both coronal heating and wind acceleration.

Evidence that the waves required to make high-speed streams do exist comes from both Doppler (Withbroe 1988) and Faraday rotation (Hollweg et al 1982) measurements. However, the validity of the interpretation of the anomalous Doppler widths has been questioned by Scudder (1992), who argued that the data could be explained by nonthermal particle distributions rather than turbulent bulk motion. The Faraday rotation measurements have been refined by Sakuri & Spangler (1995) with the result that the amplitudes are not as high as originally estimated. Recently, Coles & Esser (1992) concluded that the flows observed using radio remote sensing could not be described adequately using a wave acceleration model.

In addition to the thermal constraints on wind acceleration provided by spacecraft, important constraints are also provided by measurements of the turbulence. For example, Alfvénic fluctuations are most often observed in high-speed streams where their dissipation is most needed to accelerate the wind. However, there are large regions of slow wind that have equally Alfvénic fluctuations (Marsch et al 1981, Roberts et al 1987b), so if the presence of waves is a diagnostic of acceleration and heating, one must explain why the wind was slow in these instances. Moreover, a saturation mechanism must act continuously between a few tens of solar radii and 1 AU without destroying the Alfvénic correlations. If parametric processes were active, we would expect the fluctuations to become non-Alfvénic due to the wave scattering implicit in the interaction of the original waves with the self-generated compressive fluctuations (e.g. Viñas & Goldstein 1991a,b and references therein). The turbulent cascade mechanism must not only keep the fluctuations Alfvénic, but must also act in a region in which a strong mean magnetic field, large cross helicity, and expansion (Grappin et al 1993b) all act to slow the cascade.

The saturation picture can also be tested directly using both observations and simulations. Roberts (1989) showed that, at scales of a few hours or more, the amplitude of the fluctuations in the inner heliosphere continues to increase with distance compared to the mean field strength such that the WKB prediction holds quite well. This leaves smaller scales to account for the dissipation, presumably through a turbulence mechanism, but unless there are large features in the spectrum at high wave numbers, there cannot be enough energy available in the spectrum to do this. Although the evidence is indirect, remote sensing observations of density spectra show no evidence for large unusual spectral features at high k (Coles et al 1991, Roberts 1989). Compressible MHD simulations (Agim et al 1995; Ghosh & Goldstein 1994a,b; Roberts & Wiltberger 1995) suggest that large wave amplitudes do not initiate significant dissipation of wave energy.

5. SUMMARY

The past decade or so of research has finally established the relevance of turbulence to the evolution of interplanetary fluctuations. The free energy due to the inhomogeneity and nonstationarity of the solar atmosphere manifests itself in large-scale coherent structures such as interaction regions, but also in a general cascade of energy from large to small scales accompanied by heating. More generally, the solar wind continues to serve as an excellent laboratory for the study of nonlinear processes.

A scenario of the turbulent dynamics in the heliosphere is as follows: Either structured magnetic fields or strong velocity shears near the Sun produce a flat spectrum of fluctuations ($\approx k^{-1}$) that become largely incompressive through damping of acoustic modes and become largely outward-propagating Alfvénic fluctuations due to the “selection effect” associated with the Alfvénic critical point. The shear in the velocity field, both between and within streams, leads to approximately equal injection of power in z^+ (“outward”) and z^- (“inward”) at large scales. The low cross helicity at large scales required for this picture is due to non-Alfvénic large-scale structures and, perhaps more importantly, to the effects of the nearly spherical expansion of the flow. Because z^- is initially small at high wave numbers past the Alfvénic critical point, the low- k injection leads to a spectrum that grows until it is balanced by dissipation; both injection and dissipation then remain at a relatively low, nearly constant, level. The z^- spectrum is thus well developed, or “old,” very near the Sun. Regions where the z^- fluctuation level is high lead to stronger compressive effects, and apart from compressive structures built-in by the initial conditions at the Sun, the compressive fluctuations are largely a response to the incompressive evolution.

The injection of z^+ is inadequate to balance the rapid dissipation of the large high- k fluctuations, and thus the z^+ spectrum initially decreases rapidly. When the z^+ level is nearly equal to the z^- level, the two spectra continue to evolve slowly toward each other, with their overall amplitudes decreasing at nearly the rate they would have if no spectral transfer were occurring. Overall, the expansion may further slow the evolution; however, the turbulent evolution is accelerated in regions, such as the heliospheric current sheet at solar minimum, where the local mean field has only a small component parallel to a nearby strong shear layer. In these regions, the flat z^+ spectrum has already dissipated by 0.3 AU and thus the turbulence is more fully developed. These regions also tend to be highly structured, with sharp changes in density and other quantities, and this may contribute to the evolution both directly and possibly indirectly through the existence of strong shears near the Sun. The combined effects of dissipation and shear-driven cascades produce the evolution of spectral slopes and levels observed in the inner heliosphere. Broad slow-speed regions that do not contain a current sheet have properties similar to high-speed streams at solar minimum, and the essential difference between such slow flows and high-

speed flows is that the low-speed wind has had more time to evolve. Without the current sheet, the wind loses its Alfvénic character slowly due to a variety of causes including the nonlinear effects of small velocity shears and the (weaker) mixing effect associated with the expansion.

Any *Annual Review* chapter, as well as any article cited in an *Annual Review* chapter, may be purchased from the Annual Reviews Preprints and Reprints service.
1-800-347-8007; 415-259-5017; email: arpr@class.org

Literature Cited

- Agim YZ, Viñas AF, Goldstein ML. 1995. *J. Geophys. Res.* 100: In press
- Armstrong JW, Coles WA, Kojima M, Rickett BJ. 1990. *Ap. J.* 358:685
- Armstrong JW, Cordes, JM, Rickett BJ. 1981. *Nature* 291:561
- Barnes A. 1966. *Phys. Fluids* 9:1483
- Barnes A. 1979. In *Solar System Plasma Physics*, ed. EN Parker, CF Kennel, LJ Lanzerotti, p. 249. Amsterdam: North-Holland
- Batchelor GK. 1951. *Proc. Cambridge Philos. Soc.* 47:359
- Batchelor GK. 1970. *Theory of Homogeneous Turbulence*. New York: Cambridge Univ. Press
- Bavassano B, Bruno R. 1989. *J. Geophys. Res.* 94:11,977
- Bavassano B, Dobrowolny M, Moreno G. 1978. *Sol. Phys.* 57:445
- Bavassano M, Dobrowolny M, Fanfoni G, Mariani F, Ness NF. 1982. *Sol. Phys.* 78:373
- Belcher JW, Davis L. 1971. *J. Geophys. Res.* 76:3534
- Bieber J, Matthaeus W, Smith CW, Kallenrode, MB, Wibberenz G. 1994. *Ap. J.* 420:294
- Biskamp D, Welter H. 1989. *Phys. Fluids B* 1:1964
- Bruno R, Bavassano B, Villante U. 1985. *J. Geophys. Res.* 90:4373
- Bruno R, Bavassano B. 1991. *J. Geophys. Res.* 96:7841
- Burlaga LF, Ness NF, Belcher J, Szabo A, Isenberg P, Lee M. 1994. *J. Geophys. Res.* 99:21,511
- Burlaga LF, Ogilvie KW. 1970. *Sol. Phys.* 15:61
- Carbone V, Malara F, Veltri P. 1995. *J. Geophys. Res.* 100: In Press
- Coleman PJ. 1966. *Phys. Rev. Lett.* 17:207
- Coleman PJ. 1968. *Ap. J.* 153:371
- Coles WA, Esser R. 1992. *J. Geophys. Res.* 97:19,139
- Coles WA, Liu W, Harmon JK, Martin CL. 1991. *J. Geophys. Res.* 96:1745
- Denskat KU, Burlaga LF. 1977. *J. Geophys. Res.* 82:2693
- Dobrowolny M, Mangeney A, Veltri P. 1980a. *Phys. Rev. Lett.* 45:144
- Dobrowolny M, Mangeney A, Veltri P. 1980b. *Ap. J.* 83:2632
- Elsässer WM. 1950. *Phys. Rev.* 79:183
- Elsässer WM. 1956. *Rev. Mod. Phys.* 18:135
- Feldman WC, Gosling JT, McComas DJ, Phillips JL. 1993. *J. Geophys. Res.* 98:5593
- Freeman JW. 1988. *Geophys. Res. Lett.* 15:88
- Freeman JW, Totten T, Arya S. 1992. *EOS, Trans. Am. Geophys. Union*. Spring AGU Meet. 73:238
- Frisch U, Pouquet A, L  orat, J, Mazure A. 1975. *J. Fluid Mech.* 68:769
- Fyfe D, Montgomery D. 1976. *J. Plasma Phys.* 29:181
- Gazis PR. 1984. *J. Geophys. Res.* 89:775
- George WK, Buether PD, Arndt REA. 1984. *J. Fluid Mech.* 148:155
- Ghosh S, Goldstein ML. 1994a. *J. Geophys. Res.* 99:19,289
- Ghosh S, Goldstein ML. 1994b. *J. Geophys. Res.* 99:13,351
- Ghosh S, Matthaeus WH. 1990. *Phys. Fluids B* 2:1520
- Ghosh S, Matthaeus WH. 1992. *Phys. Fluids A* 4:148
- Ghosh S, Matthaeus WH, Montgomery D. 1988. *Phys. Fluids* 31:2171
- Ghosh S, Stribling T, Goldstein ML, Matthaeus WH. 1995. In *Space Plasmas: Coupling Between Small and Medium Scale Processes*, ed. M Ashour-Abdalla, T Chang, *Geophys. Monogr.* 86:1. Washington, DC: Am. Geophys. Union
- Goldstein B, Siscoe GL. 1972. In *Solar Wind II*, ed. CP Sonnett, JPI Coleman, JM Wilcox. *NASA Spec. Publ.* 506
- Goldstein ML, Roberts DA, Fitch CA. 1994. *J. Geophys. Res.* 99:11,519
- Goldstein ML, Roberts DA, Ghosh S, Matthaeus WH. 1987a. In *21st ESLAB Symposium*, ed. B Battrick, EJ Rolfe, p. 115. Bolkesj  : Eur. Space Agency
- Goldstein ML, Roberts DA, Matthaeus WH. 1986. *J. Geophys. Res.* 91:13,357
- Goldstein ML, Roberts DA, Matthaeus WH. 1987b. *Geophys. Res. Lett.* 14:860
- Grant HR, Stewart RW, Moilliet A. 1962. *J.*

- Fluid Mech.* 12:241
 Grappin R, Frisch U, Léorat J, Pouquet A. 1982. *Astron. Astrophys.* 105:6
 Grappin R, Mangeney A, Marsch E. 1990. *J. Geophys. Res.* 95:8197
 Grappin R, Pouquet A, Léorat J. 1983. *Astron. Astrophys.* 126:51
 Grappin R, Velli M, Mangeney A. 1991. *Ann. Geophys.* 9:416
 Grappin R, Velli M, Mangeney A. 1993a. In *Spatio-Temporal Analysis for Resolving Plasma Turbulence (START)*, p. 325. Aussois, France: Eur. Space Agency
 Grappin R, Velli M, Mangeney A. 1993b. *Phys. Rev. Lett.* 70:2190
 Heinemann M, Olbert S. 1980. *J. Geophys. Res.* 85:1311
 Higdon JC. 1984. *Ap. J.* 285:109
 Hollweg JV. 1973a. *Ap. J.* 181:547
 Hollweg JV. 1973b. *J. Geophys. Res.* 78:3643
 Hollweg JV. 1974. *J. Geophys. Res.* 79:1539
 Hollweg JV. 1975. *Rev. Geophys.* 13:263
 Hollweg JV. 1978. *Rev. Geophys.* 16:689
 Hollweg JV. 1986. *J. Geophys. Res.* 91:4111
 Hollweg JV. 1990. *J. Geophys. Res.* 95:14,873
 Hollweg JV, Bird MK, Volland H, Edenhofer P, Stelzried CT, Seidel BL. 1982. *J. Geophys. Res.* 87:1
 Hollweg JV, Johnson W. 1988. *J. Geophys. Res.* 93:9547
 Isenberg PA. 1990. *J. Geophys. Res.* 95:6437
 Jokipii JR, Kóta J. 1989. *Geophys. Res. Lett.* 16:1
 Klainerman S, Majda A. 1982. *Commun. Pure Appl. Math.* 35:629
 Klein L, Bruno R, Bavassano B. 1993a. *J. Geophys. Res.* 98:7837
 Klein L, Bruno R, Bavassano B, Rosenbauer H. 1993b. *J. Geophys. Res.* 98:17,461
 Klein LW, Roberts DA, Goldstein ML. 1991. *J. Geophys. Res.* 96:3779
 Kolmogoroff AN. 1941. *C. R. Acad. Sci. URSS* 30:301
 Koutchmy S. 1988. *Space Sci. Rev.* 47:91
 Korzhov NP, Mishin VV, Tomozov VM. 1984. *Planet. Space. Sci.* 32:1169
 Kraichnan RH. 1965. *J. Geophys. Res.* 87:6011
 Krogulec M, Musielak ZE, Suess ST, Nerney SF, Moore RL. 1994. *J. Geophys. Res.* 99:23,489
 Kunow H, Wibberenz G, Green G, Müller-Mellin R, Kallenrode M-B. 1991. In *Physics of the Inner Heliosphere*, ed. R Schwenn, E Marsch, p. 243. Heidelberg: Springer-Verlag
 Leith CE. 1967. *Phys. Fluids* 10:1409
 Lighthill MJ. 1952. *Proc. R. Soc. London Ser. A* 211:564
 Lopez RE, Freeman JW. 1982. *J. Geophys. Res.* 87:6011
 Lotova NA. 1988. *Sol. Phys.* 117:399
 Marsch E. 1991. In *Physics of the Inner Heliosphere*, ed. R Schwenn, E Marsch, p. 159. Heidelberg: Springer-Verlag
 Marsch E, Mangeney A. 1987. *J. Geophys. Res.* 92:7363
 Marsch E, Mühlhäuser K-H, Rosenbauer H, Schwenn R, Denskat KU. 1981. *J. Geophys. Res.* 86:9199
 Marsch E, Richter AK. 1987. *Ann. Geophys.* 5A:71
 Marsch E, Tu C-Y. 1989. *J. Plasma Phys.* 41:479
 Marsch E, Tu C-Y. 1990a. *J. Geophys. Res.* 95:8211
 Marsch E, Tu C-Y. 1990b. *J. Geophys. Res.* 95:11,945
 Marsch E, Tu C-Y. 1993. *J. Geophys. Res.* 98:21,045
 Matthaeus WH, Brown MR. 1988. *Phys. Fluids* 31:3634
 Matthaeus WH, Goldstein ML. 1982a. *J. Geophys. Res.* 87:6011
 Matthaeus WH, Goldstein ML. 1982b. *J. Geophys. Res.* 87:10,347
 Matthaeus WH, Goldstein ML. 1986. *Phys. Rev. Lett.* 57:495
 Matthaeus WH, Goldstein ML, King JH. 1986. *J. Geophys. Res.* 91:59
 Matthaeus WH, Goldstein ML, Montgomery DC. 1984. *Phys. Rev. Lett.* 51:1484
 Matthaeus WH, Goldstein ML, Roberts DA. 1990. *J. Geophys. Res.* 95:20,673
 Matthaeus WH, Goldstein ML, Smith C. 1982. *Phys. Rev. Lett.* 58:1256
 Matthaeus WH, Klein LW, Ghosh S, Brown MR. 1991. *J. Geophys. Res.* 96:5421
 Matthaeus WH, Lamkin SL. 1985. *Phys. Fluids* 28:303
 Matthaeus WH, Lamkin SL. 1986. *Phys. Fluids* 8:2513
 Matthaeus WH, Oughton S, Pontius D, Zhou Y. 1994. *J. Geophys. Res.* 99:19,267
 Matthaeus W, Oughton S, Pontius D, Zhou Y. 1993. *Eos, Trans. Am. Geophys. Union* 74:237
 Matthaeus WH, Zhou Y. 1989. *Phys. Fluids* B1:1929
 Miura A, Pritchett PL. 1982. *J. Geophys. Res.* 92:7431
 Moffatt HK. 1978. *Magnetic Field Generation in Electrically Conducting Fluids*. New York: Cambridge Univ. Press
 Montgomery D. 1982. *Phys. Scr.* T2/1:83
 Montgomery D. 1983. In *Theory of Hydromagnetic Turbulence*, ed. M Neugebauer, p. 107. NASA Conf. Publ. 2280
 Montgomery D, Brown M, Matthaeus WH. 1987. *J. Geophys. Res.* 92:282
 Mullan DJ. 1990. *Astron. Astrophys.* 232:520
 Oughton S. 1993. *Transport of solar wind fluctuations: a turbulence approach*. PhD thesis. Univ. Del.
 Oughton S, Matthaeus WH. 1992. In *Proc. of Solar Wind 7, COSPAR Colloq. Ser.*, ed. E Marsch, R Schwenn, p. 523. Goslar, Germany: Pergamon/Oxford Univ. Press
 Oughton S, Priest E, Matthaeus WH. 1994. *J. Fluid Mech.* Submitted

- Parker EN. 1964. *Ap. J.* 139:690
- Parker EN. 1979. *Cosmical Magnetic Fields*. Oxford: Oxford Univ. Press
- Parker EN. 1990. *Geophys. Res. Lett.* 17:2055
- Parker GD. 1980. *J. Geophys. Res.* 85:4283
- Passot T, Pouquet A. 1988. *J. Comput. Phys.* 75:300
- Pontius D, Gray P, Hossain M, Matthaeus W. 1993. *Eos, Trans. Am. Geophys. Union* 74:477
- Pouquet A, Frisch U, Léorat J. 1976. *J. Fluid Mech.* 77:321
- Roberts DA. 1989. *J. Geophys. Res.* 94:6899
- Roberts DA. 1990. *J. Geophys. Res.* 95:1087
- Roberts DA. 1992. In *Proc. of Solar Wind 7, COSPAR Colloq. Ser.*, ed. E Marsch, R Schwenn, p. 533. Goslar, Germany: Pergamon/Oxford Univ. Press
- Roberts DA, Wiltberger MJ. 1995. *J. Geophys. Res.* 100:3405
- Roberts DA, Ghosh S, Goldstein ML, Matthaeus WH. 1991. *Phys. Rev. Lett.* 67:3741
- Roberts DA, Goldstein ML. 1991. In *U. S. National Report to International Union of Geodesy and Geophysics*, ed. MA Shea, p. 932. Washington, DC: Am. Geophys. Union
- Roberts DA, Goldstein ML, Klein LW. 1990. *J. Geophys. Res.* 95:4203
- Roberts DA, Goldstein ML, Klein LW, Matthaeus WH. 1987a. *J. Geophys. Res.* 92:12,023
- Roberts DA, Goldstein ML, Matthaeus WH, Ghosh S. 1992. *J. Geophys. Res.* 97:17,115
- Roberts DA, Goldstein ML, Matthaeus WH, Klein LW. 1989. In *Turbulence and Nonlinear Dynamics in MHD Flows*, eds. M Meneguzzi, A Pouquet, PL Sulem, p. 87. Amsterdam: Elsevier
- Roberts DA, Klein LW, Goldstein ML, Matthaeus WH. 1987b. *J. Geophys. Res.* 92:11021
- Robinson DC, Rusbridge MG. 1971. *Phys. Fluids* 14:2499
- Robinson DC, Rusbridge MG, Saunders PA. H. 1968. *J. Plasma Phys.* 10:1005
- Rusbridge MG. 1969. *J. Plasma Phys.* 11:35
- Sakurai T, Spangler SR. 1995. *Ap. J.* In press
- Sari JW, Valley GC. 1976. *J. Geophys. Res.* 81:5489
- Schwenn R. 1983. In *Solar Wind Five, NASA Conf. Publ.* CP-2280:485
- Scott SL, Coles WA, Bourgois G. 1983. *Astron. Astrophys.* 123:207
- Scudder JD. 1992. *Ap. J.* 398:319
- Shebalin JV, Matthaeus WH, Montgomery D. 1983. *J. Plasma Phys.* 29:525
- Shebalin JV, Montgomery D. 1988. *J. Plasma Phys.* 39:339
- Solodyna CV, Belcher JW. 1976. *Geophys. Res. Lett.* 3:565
- Southwood DJ. 1968. *Planet. Space Sci.* 16:587
- Strauss HR. 1976. *Phys. Fluids* 19:134
- Stribling T, Matthaeus WH. 1995. In *Space Plasmas: Coupling Between Small and Medium Scale Processes*, ed. M Ashour-Abdalla, T Chang, *Geophys. Monogr.* 86:55. Washington, DC: Am. Geophys. Union
- Stribling T, Matthaeus WH, Ghosh S. 1994. *J. Geophys. Res.* 99:2567
- Stribling T, Matthaeus WH, Oughton S. 1995a. *Phys. Fluids B* In press
- Stribling T, Roberts DA, Goldstein ML. 1995b. *J. Geophys. Res.* Submitted
- Ting AC, Matthaeus WH, Montgomery C. 1986. *Phys. Fluids* 3261
- Tu C-Y. 1987. *Sol. Phys.* 109:149
- Tu C-Y. 1988. *J. Geophys. Res.* 93:7
- Tu C-Y, Marsch E. 1990a. *J. Geophys. Res.* 95:4337
- Tu C-Y, Marsch E. 1990b. *J. Plasma Phys.* 44:103
- Tu C-Y, Marsch E. 1991. *Ann. Geophys.* 9:319
- Tu C-Y, Marsch E. 1992. In *Proc. of Solar Wind 7, COSPAR Colloq. Ser.*, ed. E Marsch, R Schwenn, p. 549. Goslar, Germany: Pergamon/Oxford Univ. Press
- Tu C-Y, Marsch E. 1993. *J. Geophys. Res.* 98:1257
- Tu C-Y, Marsch E, Rosenbauer H. 1990. *Geophys. Res. Lett.* 17:283
- Tu C-Y, Pu Z-Y, Wei F-S. 1984. *J. Geophys. Res.* 89:9695
- Unti TW, Neugebauer M. 1968. *Phys. Fluids* 11:563
- Vellante M, Lazarus AJ. 1987. *J. Geophys. Res.* 92:9893
- Velli M. 1993. *Astron. Astrophys.* 270:304
- Velli M, Grappin R, Mangeney A. 1989. *Phys. Rev. Lett.* 63:1807
- Velli M, Grappin R, Mangeney A. 1991. *Astrophys. Fluid Dyn.* 62:101
- Verma M, Roberts DA. 1993. *J. Geophys. Res.* 98:5625
- Verma M, Roberts DA, Goldstein ML. 1995. *J. Geophys. Res.* 100: Submitted
- Verma MK. 1994. *Magnetohydrodynamic turbulence models of solar wind evolution*. PhD thesis. Univ. MD, College Park
- Viñas AF, Goldstein ML. 1991a. *J. Plasma Phys.* 46:129
- Viñas AF, Goldstein ML. 1991b. *J. Plasma Phys.* 46:107
- Völk HJ, Alpers W. 1973. *Astrophys. Space Sci.* 20:267
- Whang YC, Burlaga LF. 1985. *J. Geophys. Res.* 90:10,765
- Whang YC, Liu S, Burlaga LF. 1991. *J. Geophys. Res.* 95:18,769
- Withbroe GL. 1988. *Ap. J.* 325:442
- Woltjer L. 1958. *Proc. Natl. Acad. Sci. USA* 44:833
- Woo R, Schwenn R. 1991. *J. Geophys. Res.* 96:21,227
- Woo RW, Armstrong JW. 1979. *J. Geophys. Res.* 84:7288

- Zank GP, Matthaeus WH. 1990. *Phys. Rev. Lett.* 64:1243
- Zank GP, Matthaeus WH. 1991. *Phys. Fluids A* 3:69
- Zank GP, Matthaeus WH. 1992a. *Phys. Fluids A* In Press
- Zank GP, Matthaeus WH. 1992b. *J. Geophys. Res.* 97:17,189
- Zank GP, Matthaeus WH, Klein LW. 1990. *Geophys. Res. Lett.* 17:1239
- Zank G, Matthaeus W. 1993. *Phys. Fluids A* 5:257
- Zhou Y, Matthaeus WH. 1989. *Geophys. Res. Lett.* 16:755
- Zhou Y, Matthaeus WH. 1990a. *J. Geophys. Res.* 95:14,881
- Zhou Y, Matthaeus WH. 1990b. *J. Geophys. Res.* 95:14,863
- Zhou Y, Matthaeus WH. 1990c. *J. Geophys. Res.* 95:10,291
- Zhou Y, Matthaeus WH, Roberts DA, Goldstein ML. 1990. *Phys. Rev. Lett.* 64:2591
- Zweiben SJ, Menyuk CR, Taylor RJ. 1979. *Phys. Rev. Lett.* 42:1270
- Zweiben SJ, Taylor RJ. 1981. *Nucl. Fusion* 21:193